Clay-mineral distribution in recent deep-sea sediments around Taiwan: Implications for sediment dispersal processes

Kalyani Nayak [a,b], Andrew Tien-Shun Lin [a,b,*], Kuo-Fang Huang [a,c], Zhifei Liu [d], Nathalie Babonneau [e], Gueorgui Ratzov [f], Radha Krishna Pillutla [a,b], Prabodha Das [b], Shu-Kun Hsu [a,b]

[a] Earth System Science Program, Taiwan International Graduate Program, Academia Sinica and National Central University, Taiwan
[b] Department of Earth Sciences, National Central University, Taiwan
[c] Institute of Earth Sciences, Academia Sinica, Taiwan
[d] State Key Laboratory of Marine Geology, Tongji University, Shanghai, China
[e] UMR6538 Laboratoire Geosciences Océan, IUEM, Université de Brest, France
[f] Université Côte d'Azur, CNRS, Observatoire de la Côte d'Azur, IRD, Géoazur, Nice, France

ARTICLE INFO

ABSTRACT

Clay-mineralogy study of Taiwanese river-mouth sediments, recent deep-water seafloor sediments around Taiwan, along with sediments collected from the Tainan shelf edge, have been investigated to access the source and transport of detrital fine-grained sediments. We determined the clay mineralogy in both hemipelagites and turbidites in the top 50 cm of the deep-sea sediment cores to infer how sediments are dispersed through river-fed turbidity currents, hypopycnal plumes, and oceanic currents. Our results show that the clay mineral assemblages in both hemipelagites and turbidites of different provinces change gradually between two major end-members: illite+chlorite and smectite. They are predominantly sourced from Taiwan and Luzon, respectively. The relative abundances of clay minerals in turbidites and hemipelagites are quite similar in most of the cores. Therefore, we argue that the adjacent turbidites and hemipelagites of a core share common detrital clay sources. We found that smectite is relatively abundant around Taiwan, indicating that the Kuroshio Current is an important transportation system, which brings smectite from Luzon. Besides, the river-related canyon systems consist dominantly of illite and chlorite, and less smectite, indicating that the smectite brought about by the Kuroshio Current is diluted by river-fed hyperpycnal and hypopycnal flows. This also implies that flood-induced turbidity currents are efficient agents for transporting Taiwan-derived sediments into the neighboring deep-sea basins. The

1. Introduction

The provenance study of detrital sediments in the ocean is essential for a better comprehension of environment and climate interactions that occurred in nearby land source areas. Climatic variability and tectonics were regarded to be the primary controlling variables for erosion on different geological timescales, though their comparative roles are still heavily debated (Burbank et al., 2003; Clift et al., 2006; Dadson et al., 2003; Liu et al., 2007b; Molnar, 2004; Peizhen et al., 2001; Reiners et al., 2003). High sediment discharge and tectonic elevation in tropical southeast Asia make river basins important areas for studying variables that regulate weathering (Dadson et al., 2003; Huang et al., 2016; Milliman et al., 1999; Milliman and Syvitski, 1992). Such discussion further

strengthened the need for a better comprehension of the variables controlling weathering and erosion in mountain ranges and the largest river basins in the world (Canfield, 1997; Gaillardet et al., 1999; Kandasamy and Chen, 2006; Liu et al., 2007b; McLennan, 1993; Milliman and Syvitski, 1992; Singh et al., 2005; Summerfield and Hulton, 1994).

Taiwan is known to be an area with one of the world's highest sediment yields (Dadson et al., 2003; Li et al., 2011). The variability and intensity of the processes controlling sediment transport around Taiwan, which include frequent typhoons, heavy rainfall, strong tectonic activity, and intense oceanic circulation, make it an ideal area to study the effect of these processes on sediment transfer to the deep-sea. This paper, therefore, seeks to understand how different variables play a role in the distribution of detrital fine-grained sediments around Taiwan. The

offshore areas around Taiwan receive detrital sediments from various sources including the Taiwan Island, rivers in southeast China (e.g., the Jiulong River and Pearl River, specifically supplying sediments to offshore southwest Taiwan), the Luzon Islands, and the Ryukyu Islands through various sedimentary processes (Fig. 1). Deep-water sediments around offshore Taiwan are dominated by hemipelagites and gravity-flow deposits. This may lead to different clay mineral distributions in offshore Taiwan, where it encompasses various types of tectonic settings and basins.

There have been a few studies using clay mineralogy to unravel the sediment source-to-sink for the seafloor sediments in the Northeast South China Sea (NE SCS) e.g., (Liu et al., 2010b; Liu et al., 2008b; Wan et al., 2007). However, no study has been done using clay minerals as tracers to study sediment source-to-sink in offshore eastern Taiwan, in the upper-slope of the Manila accretionary wedge, and the Luzon forearc basin. We study clay mineralogy to unravel the source-to-sink movement of recent deep-sea sediments around Taiwan, including the Ryukyu subduction zone, Huatung Basin in the Philippine Sea Plate, the Manila subduction zone, and the rifted continental margin of the NE South China Sea near Taiwan (Figs. 1b, 2). We focused on determining the changes in clay mineral distributions in different sedimentary facies (hemipelagites and turbidites, in particular) in the top 50 cm of seafloor

sediments around Taiwan to understand the sediment dispersal processes. River-mouth samples from 31 Taiwanese rivers and a few grabbed surface sediment samples from southern Taiwan Strait (Tainan Shelf) were collected and analyzed for a better understanding of the sediment sources.

The objectives of this research are:

1) To explore the sedimentary processes responsible for various deep-sea sediment facies around Taiwan.
2) To unravel the distribution patterns of clay minerals in different sedimentary facies of deep-sea surface sediments.
3) To decipher how sediments are dispersed through river-fed turbidity currents, hypopycnal plumes, and oceanic currents, more specifically the Kuroshio Current, around Taiwan.

2. Geological setting and environmental background

Taiwan is situated at the tectonic collision boundary between the Philippine Sea Plate and the Eurasian Plate, leading to a rapid uplift rate of 5–7 mm/a in the Taiwan orogen (Dadson et al., 2003; Li et al., 2011). The Taiwan orogen connects two opposite dipping subduction systems: the Manila subduction zone to the south where the South China Sea
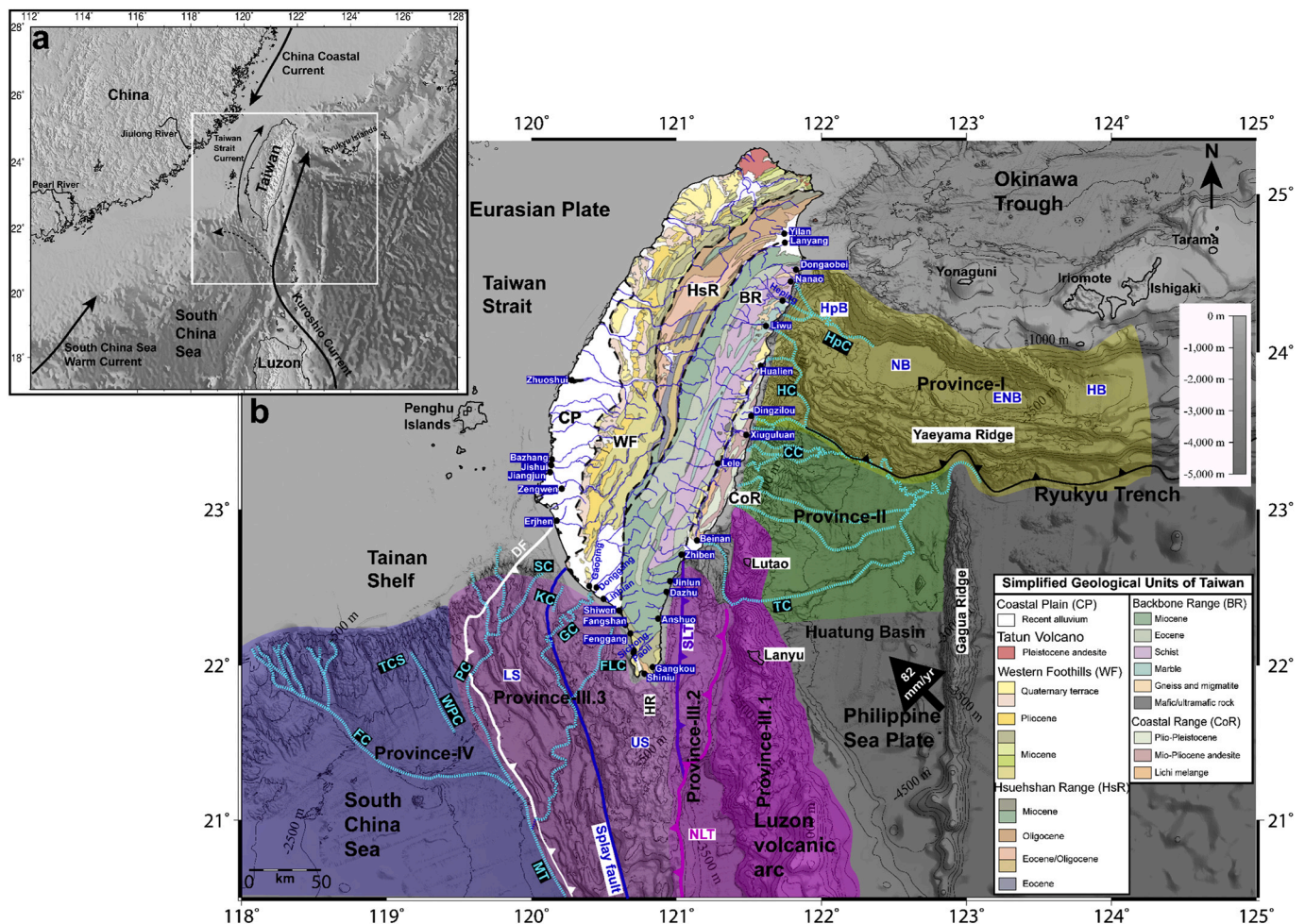

Fig. 1. (a) Map of Taiwan and its vicinity showing the oceanic current flow patterns. The location of the study area is marked by a white rectangle. (b) Geological map of Taiwan (after Chen, 2000) and shaded relief bathymetry offshore Taiwan. Major faults, canyons, and river sediment sampling locations (black circles) are shown on this map. The classified provinces are marked with different colours. Abbreviations: BR: Backbone Range, CC: Chimei Canyon, CoR: Coastal Range, CP: Coastal Plain, DF: Deformation Front, ENB: East Nanao Basin, FLC: Fangliao Canyon, FC: Formosa Canyon, GC: Gaoping Canyon, HB: Hateruma Basin, HC: Hualien Canyon, HP: Hengchun Peninsula, HR: Hengchun Ridge, HpB: Hoping Basin, HpC: Hoping Canyon, HsR: Hsuehshan Range, KC: Kaohsiung Canyon, MT: Manila Trench, NB: Nanao Basin, NLT: North Luzon Trough, PC: Penghu Canyon, SC: Shousan Canyon, SLT: Southern Longitudinal Trough, TC: Taitung Canyon, TCS: Tainan Continental Slope, WF: Western Foothills, WPC: West Penghu Canyon and the splay fault bordering the lower-slope (LS) and upper-slope(US) domains.
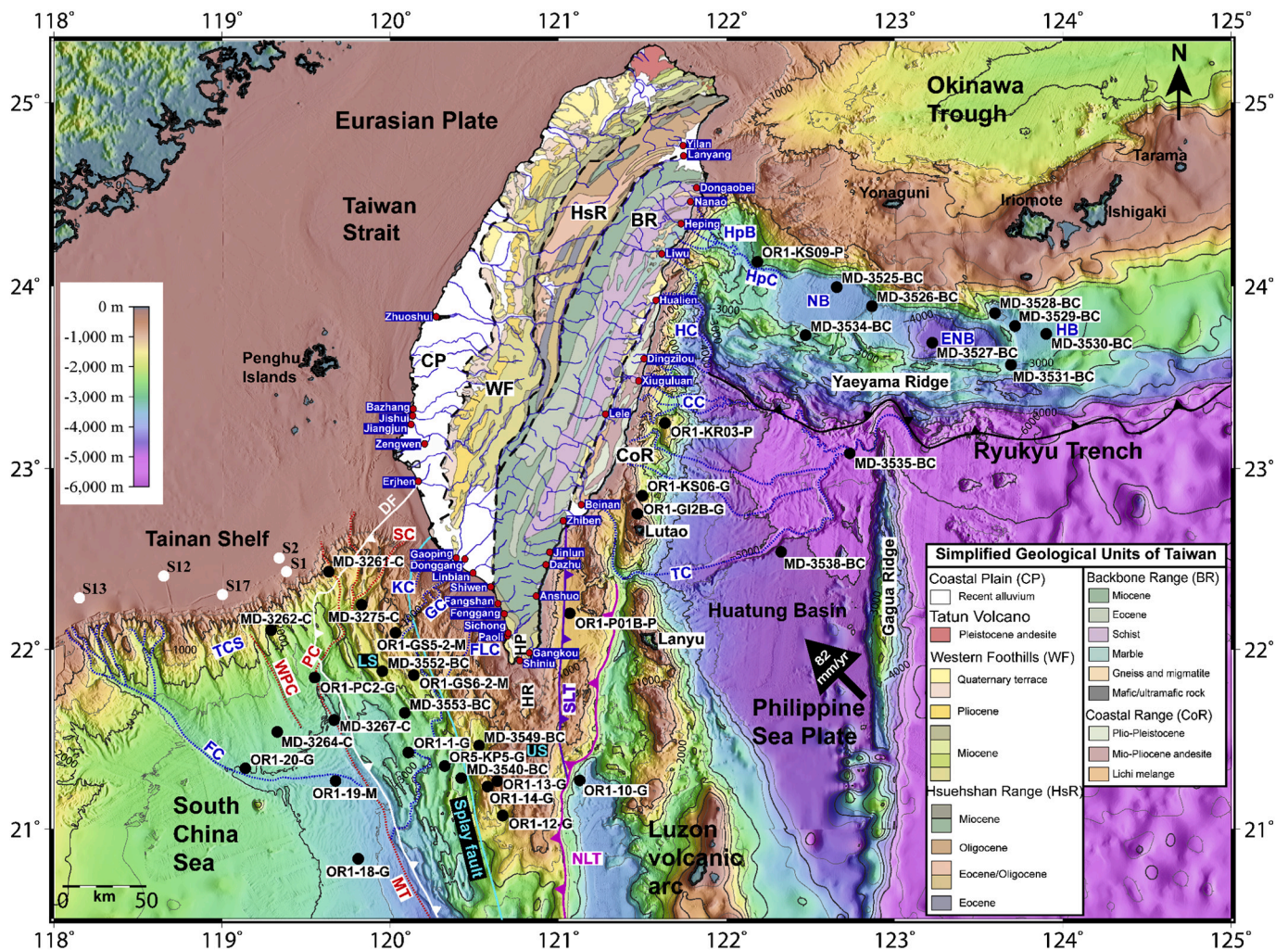
Fig. 2. Shaded relief bathymetric map around offshore Taiwan, showing Major faults, canyons, location of sediment cores (black circles), and location of sediment grabs from the southern Taiwan Strait (white circles). Geological map of Taiwan showing river sediment sampling locations (red circles). See Fig. 1 for abbreviations. (For interpretation of the references to colour in this figure legend, the reader is referred to the web version of this article.)

lithosphere is being subducted eastwards beneath the Philippine Sea Plate, building an accretionary wedge; and the Ryukyu subduction zone to the northeast where the Philippine Sea Plate subducts beneath the Eurasian Plate. The Taiwan Island experiences roughly four typhoons per year with nominal annual precipitation of 2500 mm/yr along with frequent earthquakes, resulting in rapid mass-wasting and fluvial incision (Dadson et al., 2003; Huang et al., 2016). Taiwanese rivers currently have annual discharges of roughly 180–380 Mt. of sediments into the surrounding waters (Dadson et al., 2003; Kao and Milliman, 2008; Li et al., 2011). This suggests that Taiwan is a significant source of sediments for the studied region.

Taiwan-derived sediments are transported to the surrounding deep seas through an array of submarine canyons. For example, the Penghu Canyon, Shoushan Canyon, Kaohsiung Canyon, Gaoping Canyon, and Fangliao Canyon (from north to south) off southwest Taiwan, deliver a vast amount of sediment from southwest Taiwan (Fig. 1b). Among these canyons, the river-connected Gaoping Canyon plays a major role in transferring terrestrial sediments from mountainous catchments to the deep-sea through episodic gravity flows and hyperpycnal flows (Liu et al., 2016a; Liu, 2002; Selvaraj et al., 2015; Sparkes et al., 2015; Yu et al., 2017; Zhang et al., 2018). The Gaoping River delivers a higher amount of sediments to the adjacent sea (~40–50 Mt./a, Dadson et al., 2003), compared to other southwest Taiwan rivers. In the eastern part of Taiwan, the drainage systems associated with three main submarine

canyons (the Hualien Canyon, Chimei Canyon, and Taitung Canyon from north to south, which reach into the mouths of the Hualien, Xiuguluan, and Beinan rivers, respectively; Hsieh et al., 2020) receive terrestrial sediments discharged from eastern Taiwan (Fig. 1b). The sediment delivery of the Hualien River (19–31 Mt./a), the Xiuguluan River (16–22 Mt./a), and the Beinan River (17–88 Mt./a) are higher among other eastern Taiwan rivers (Dadson et al., 2003; Liu et al., 2008a), indicating river-connected canyon systems play an important role in transferring Taiwan derived sediments into adjacent deep-seas. Besides, many submarine channels, which seem not connected with subaerial drainage systems, engrave the continental slope and amalgamate with the submarine canyons, suggesting prevalent marine erosional processes. This indicates that seafloor sediment remobilization is also common in the study area.

The deep-sea sediments around Taiwan are mostly sourced from Taiwan Island with illite and chlorite as characteristic clay minerals for seafloor sediments as seen in sediment cores in NE SCS (Dadson et al., 2003; Liu et al., 2010a; Liu et al., 2008b; Wan et al., 2007). However, surface oceanic currents play an important role in dispersing fine-grained sediments in deep-water settings. The Kuroshio Current is the major surface oceanic current offshore around Taiwan (Mensah et al., 2015). In winter, a branch of this current, named the Kuroshio Intrusion, is observed flowing from offshore northeast Luzon to off southwest Taiwan and then westward along the northern continental slope of the

SCS; while in summer, it deviates from the winter trail to the south (Fig. 1a; Liu et al., 2010b; Yuan et al., 2006). In offshore eastern Taiwan, the main Kuroshio Current turns to the east towards the Okinawa Trough after passing along and off the coast of Taiwan (Fig. 1a). This significant oceanic current, therefore, plays a major role in transporting suspended material around offshore Taiwan (e.g., Kaifu et al., 2020). Specifically, the Kuroshio Current brings fine-grained sediments from the Luzon Islands (Liu et al., 2008b).

3. Materials and methods

3.1. Sample collection

A set of 36 deep-sea sediment cores from eastern, southern, and southwestern offshore parts of Taiwan, together with 31 river-mouth sediment samples from major Taiwanese rivers and 5 grabbed surface sediment samples from southern Taiwan Strait (near the shelf edge called Tainan Shelf) were collected for this study (Fig. 2). The gravity (G), piston (P), calypso-piston (C), and box (BC) cores were collected onboard R/V *Ocean Researcher I* during OR1–891, OR1–1013, OR1–1048, OR1–1138, OR5–0032 cruises and onboard R/V *Marion Dufresne* during MD178, MD214 EAGER cruises (Table S1). The sediment grabs from the southern Taiwan Strait (sites S1, S2, S12, S13, S17) were obtained during OR3–1938 cruise. In terms of the tectonic framework, the locations of all studied sediment cores are divided into four major provinces: (I) Ryukyu subduction zone, (II) Huatung Basin of the Philippine Sea Plate, (III) Manila subduction zone and Luzon volcanic arc, and (IV) NE South China Sea (Fig. 1b). The main provinces are further subdivided into small subgroups according to bathymetry and possible sediment delivery processes (Table S1).

3.2. Analytical methods

All the sediment cores were split into two equal halves as working and archive halves. The archive halves were visually described to comprehend the sedimentary features in the cores. The working halves were sampled at 1-cm intervals and the samples were freeze-dried in centrifuge tubes for further analyses. Measurements of non-destructive physical properties (i.e., gamma density, P-wave velocity, porosity,

and magnetic susceptibility) at 1-cm intervals were performed using a Multi-Sensor Core Logger (MSCL) onboard for the cores retrieved during MD214 EAGER cruise and at the Taiwan Ocean Research Institute for the cores retrieved during OR1–1013, OR1–1048, OR1–1138, OR5–0032, MD178 cruises.

Grain size pre-treatment processes were done for all dried sediment samples using 15% hydrogen peroxide and 10% hydrochloride for 1–2 days to remove organic matters and carbonates, respectively. Sodium hexametaphosphate was added to all the samples and they were put in an ultrasonicator to deflocculated and disperse sediment grains before carrying out grain size analyses using a Beckman Coulter LS13 320 laser diffraction particle-size analyzer at the Sediment Analysis Lab of the National Central University (SALNCU), which can analyze grains between 0.017 μm and 2000 μm.

We delineated the variability of sedimentary facies based on both sedimentological data such as visual description, MSCL results (P-wave velocity and gamma density), and grain-size data such as grain-size volume distribution pattern, median, sorting, kurtosis, and skewness (Fig. 3, Figs. S1-S13). Sediments were described with special attention to distinguish turbidites from hemipelagites. The definition of hemipelagite facies can be found in Stow and Tabrez (1998) and in our studied cores it consists of homogeneous silty-clay with dispersed foraminifera and occasional vague laminations. They are typically marked by the finest median grain-size ($\leq$ 10 μm, Lehu et al., 2015). The turbidite facies is primarily identified by its coarser grain-size with higher median values (>10 μm), and an upward-fining trend (Fig. 3). Turbidites are commonly interbedded with hemipelagites. The base of each turbidite layer is commonly marked by an erosive surface or sharp boundary with noticeable breaks in grain-size and sediment colour.

In order to analyze clay mineralogy, we selected 1 to 2 cm of sediment segments at different intervals, depending on changes in sedimentary facies from both turbidites and hemipelagic deposits in the top 50 cm of the cores. Clay minerals were identified by X-ray diffraction (XRD) using a Bruker D2 Phaser X-ray diffractometer at SALNCU. For clay mineral analysis, the bulk sediments were pretreated with hydrogen peroxide (10%) and acetic acid (15%) to remove organic matter and carbonates, respectively. Then, the clay fraction (< 2um) was segregated from the bulk sediment solution based on conventional Stokes' settling velocity principles and centrifuged. Each sample was transmitted by
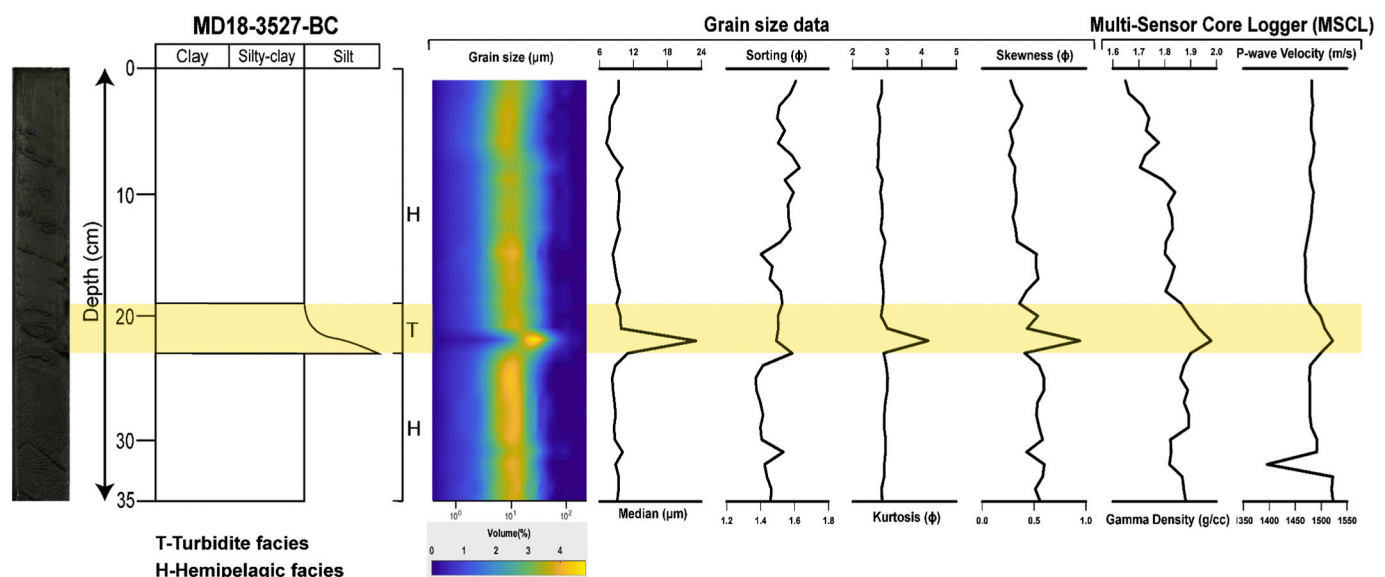

Fig. 3. Representative figure for identification of turbidites (T) and hemipelagites (H) of a sediment core using core photo, lithological descriptions, grain-size data (grain-size volume distribution pattern, median, sorting, kurtosis, and skewness), and petrophysical characteristics (P-wave velocity and gamma density) from MSCL. See supplementary figures for other cores. The shaded yellow areas indicate the turbidite layers. (For interpretation of the references to colour in this figure legend, the reader is referred to the web version of this article.)

moist smearing to slides and was kept for air-drying. XRD runs were then carried out three times following air-drying, ethylene–glycol solvation, and heating at 490 °C for 2 h. The identification of clay minerals was based primarily on the position of the (001) series of basal reflections on the three XRD diagrams (Fig. 4). A few chosen ethylene glycolated XRD curves from different provinces were used to perform a qualitative analysis of clay minerals for comparison (Fig. 5).

Semi-quantitative estimates of basal reflection peak areas for major mineral groups of smectite (15–17 Å, including mixed-layers of smectite-illite at 15–16 Å), illite (10 Å), and kaolinite+chlorite (7 Å) were performed on glycolated specimens using PeakFit software after background subtraction. Relative proportions of kaolinite and chlorite were determined using the ratio at the 3.57/3.54 Å peak area. Weighting factors introduced by Biscaye (1965) or Holtzapffel (1985) are not used in this study to produce comparative weight percentages of each clay mineral, because such regular weighting factors do not occur through systemic experiences (Liu et al., 2010b). Replicate analyses of a few chosen samples gave ±3% accuracy. Clay mineral data from prior studies (Liu et al., 2007b; Liu et al., 2009) of the Pearl River and Luzon rivers, where they applied the same method to calculate the relative percentage of the main four clay minerals were used in this study for comparison and to track the source regions.

The illite crystallinity was calculated as the full width at half maximum (FWHM) of the illite 10 Å peak and the illite chemical index was estimated using a ratio of 5 Å and 10 Å peak areas for ethylene-glycolated samples. Both parameters are helpful in identifying sources of sediments and their transport routes (Diekmann and Wopfner, 1996; Li et al., 2011); Gingele et al., 2001; Gingele, 1996; Kuo et al., 2012; Liu et al., 2007a; Wan et al., 2010).

4. Results

4.1. Sediment facies for seafloor sediments

Based on both sedimentological data and grain-size data, we distinguished two end-member sediment facies (turbidite and hemipelagite facies) for the studied cores from different provinces around Taiwan (Fig. 3, Figs. S1-S13). Most of the studied cores are characterized by both facies. For example, the core MD18–3527-BC, located in the East Nanao

Basin, consisting of both hemipelagites and turbidite (Fig. 3). Nearly 1/4 of the studied cores are composed mainly of homogeneous silty-clay, pertaining to hemipelagic deposits (Figs. 6, 7, 8, 9, 10, 11).

Our results show that more turbidites are found in the canyon-related depositional systems (e.g., Taitung, Gaoping, and Formosa Canyons; Figs. 7, 10, 11). Frequent turbidite layers are also found in the deformed forearc basin in the Southern Longitudinal Trough as well as in some perched basins in the upper slope of the Manila accretionary wedge (Figs. 8, 9). Hemipelagites are found particularly away from the canyons, on bathymetric highs, and some perched basins in accretionary wedges (Figs. 6, 7, 8, 9).

4.2. Distribution of clay minerals in Taiwanese river sediments and Tainan Shelf sediments

The clay fraction (< 2 um) of the studied Taiwanese river-mouth sediments consist mainly of illite (32%–76%, with an average of ~60%) and chlorite (13%–58%, with an average of ~30%) with no or a small amount of kaolinite and smectite (Table S2). A few rivers contain very scarce to a small amount of smectite (≤ 8%) such as the Yilan, Lanyang, Dongaobei, Heping, Liwu, Hualien, Lele, Beinan, Zhiben, Gangkou, and Zhuoshui rivers. Minor to moderate amounts of smectite (10–19%) are found in the Erjhen, Zengwen, Jiangjun, Jishui, and Bazhang rivers in southwest Taiwan. Two rivers in the Coastal Range (the Dingzilou and Xiuguluan rivers) contain higher amounts of smectite (53% and 40%, respectively).

The average contents of chlorite are greater in eastern Taiwan (~33%) than in western Taiwan (~27%). The abundance of chlorite in the Dongaobei, Liwu, Hualien, and Nanao rivers is as high as 58%, 48%, 47%, and 44%, respectively (Table S2). The kaolinite contents of the Gangkou, Shiniu, Paoli, Sichong, Erjhen, Jiangjun, and Bazhang rivers are varied in the range from around 8% to 12% with an average value of about ~10%. The Gangkou, Shiniu, Paoli, and Sichong rivers are located in the Hengchun Peninsula, the southern tip of Taiwan, whereas the Erjhen, Jiangjun, and Bazhang rivers are located in southwest Taiwan (Fig. 2). However, the kaolinite contents vary in the range of 0–7% in other rivers in southwest Taiwan and 0–3% in the east Taiwan Rivers. Illite crystallinity and illite chemistry index of the river sediments vary in the range of 0.17°–0.43°Δ2θ and 0.18–0.35, respectively. The illite
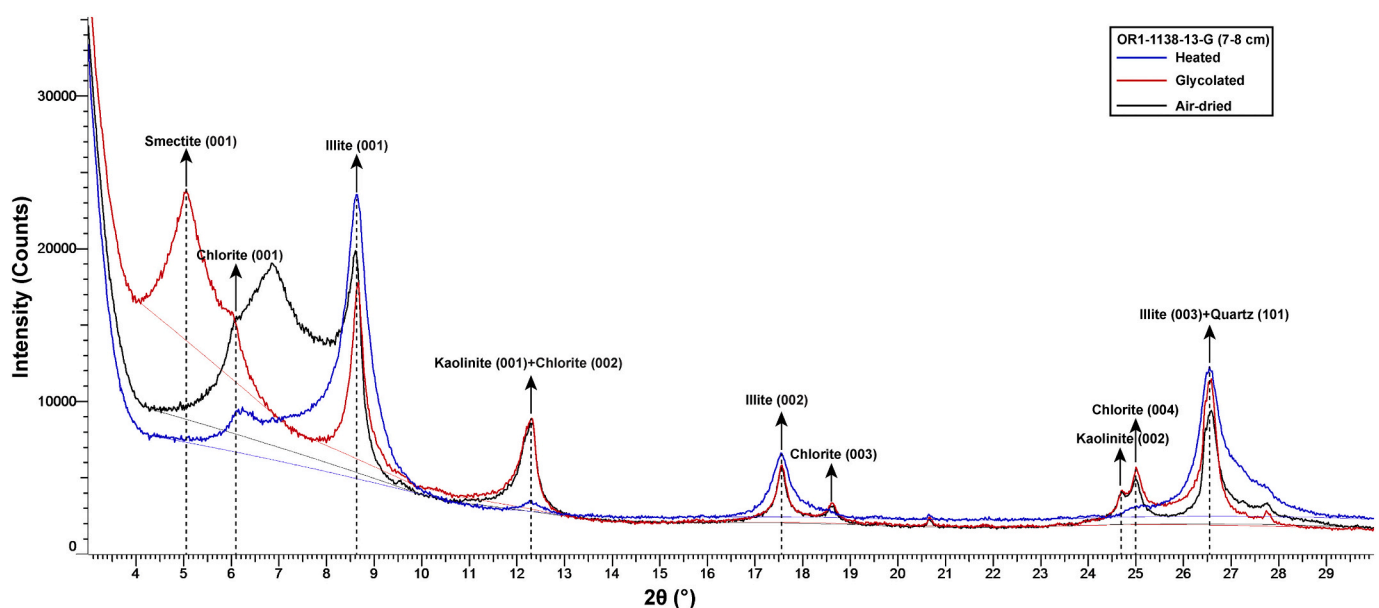

Fig. 4. Representative X-ray diffraction pattern of <2 μm fractions of a particular interval from a cored sediment sample. Black, red, and blue lines are the results of air-dried, ethylene glycol solvation, and heated samples, respectively. (For interpretation of the references to colour in this figure legend, the reader is referred to the web version of this article.)
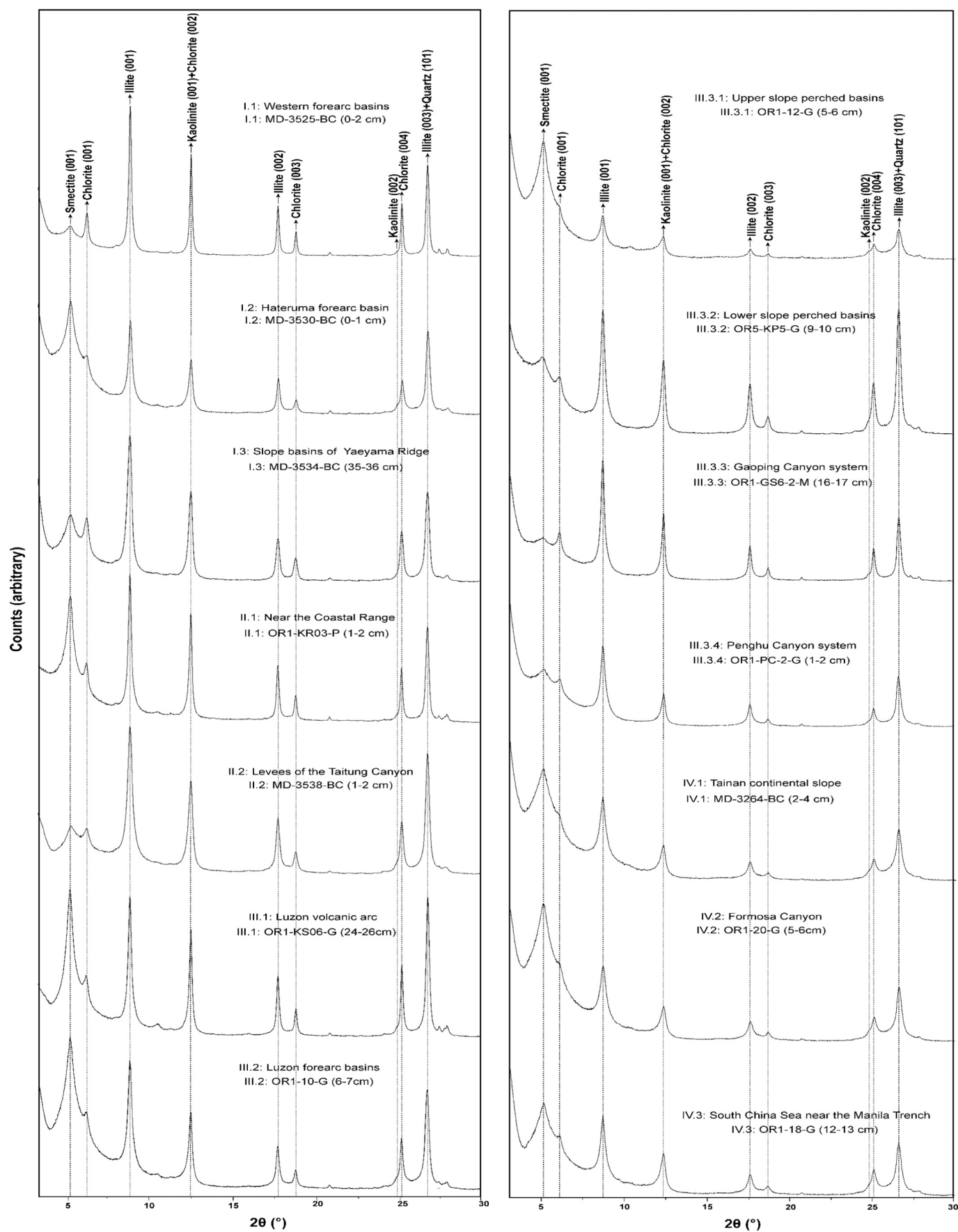
Fig. 5. Glycolated X-ray diffraction patterns of representative samples from different provinces.
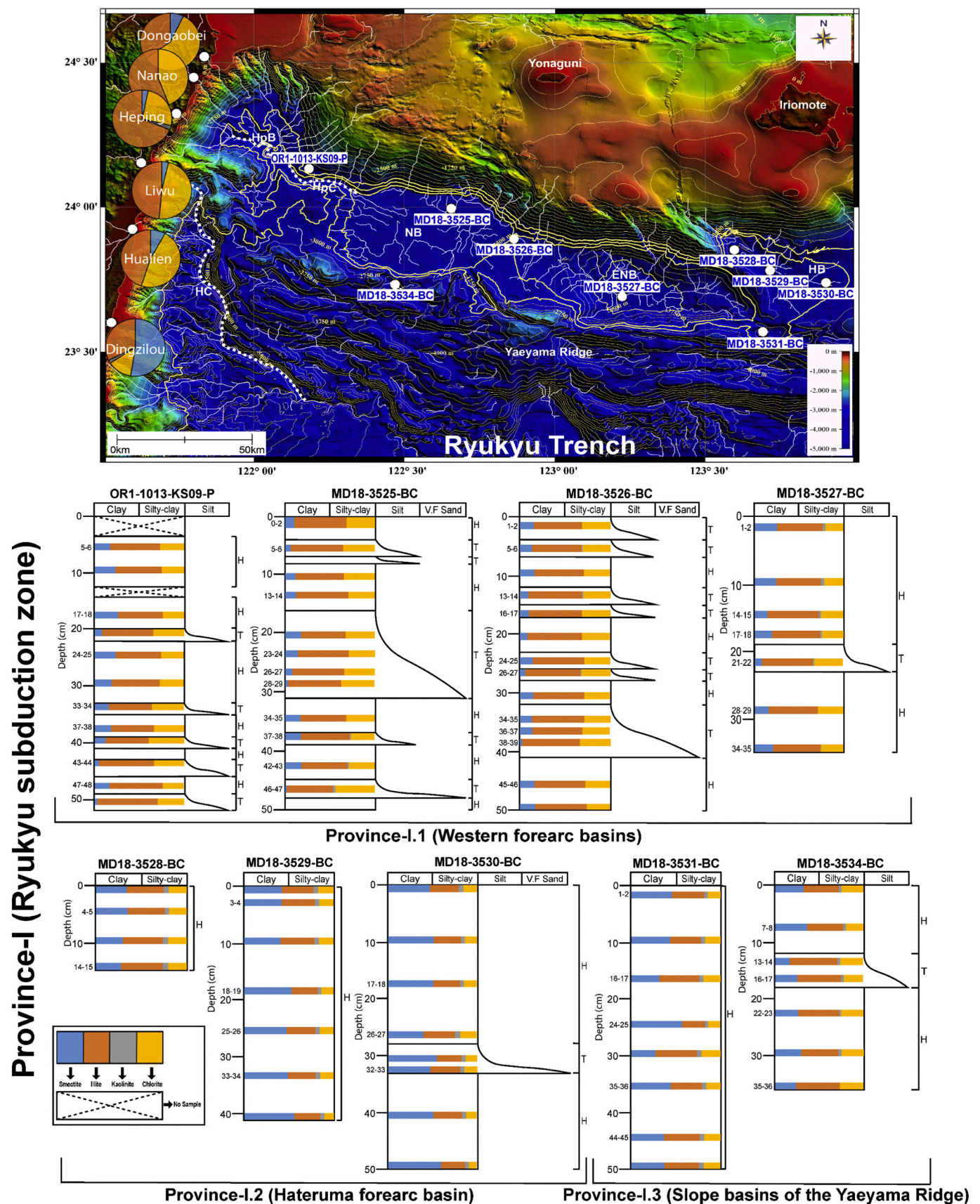
Fig. 6. Figure showing drainage patterns with distributions of clay mineral percentages in surrounding Taiwanese river sediments and lithological descriptions with vertical clay mineral distributions of the studied cores in Province-I. Abbreviations: ENB: East Nanao Basin, HB: Hateruma Basin, HC: Hualien Canyon, HpB: Hoping Basin, HpC: Hoping Canyon, NB: Nanao Basin. *Contour lines* show the elevation in *250-m intervals.*
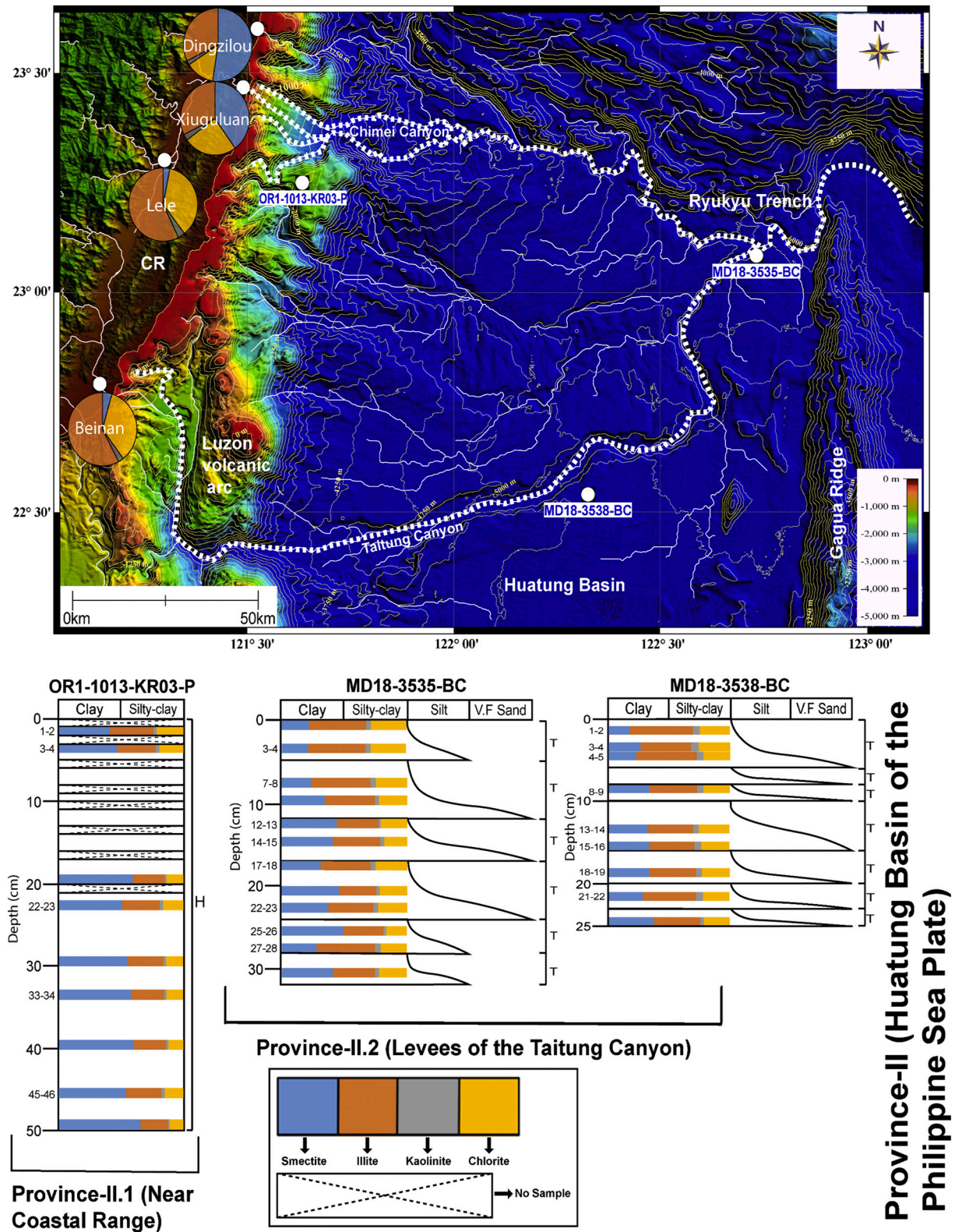
Fig. 7. Figure showing drainage patterns with distributions of clay mineral percentages in surrounding Taiwanese river sediments and lithological descriptions with vertical clay mineral distributions of the studied cores in Province-II. Abbreviation: CR: Coastal Range. *Contour lines* show the elevation in *250-m intervals.*

chemistry index for the sediments from all the Taiwanese rivers is less than 0.35, indicating that illite in Taiwan is mainly Fe-Mg rich.

The clay-mineral assemblages of the Tainan Shelf sediments (Table S3) consist mainly of illite (38–54%, with an average of 47%) with moderate amounts of smectite (16–38%, with an average of ~24%)

and chlorite (17–22%, with an average of ~21%), and minor amounts of kaolinite (7–9%, with an average of ~8%). Illite crystallinity and illite chemistry index of the sediments vary in the range of 0.26°–0.33°$\Delta 2\theta$ and 0.27–0.39, respectively.
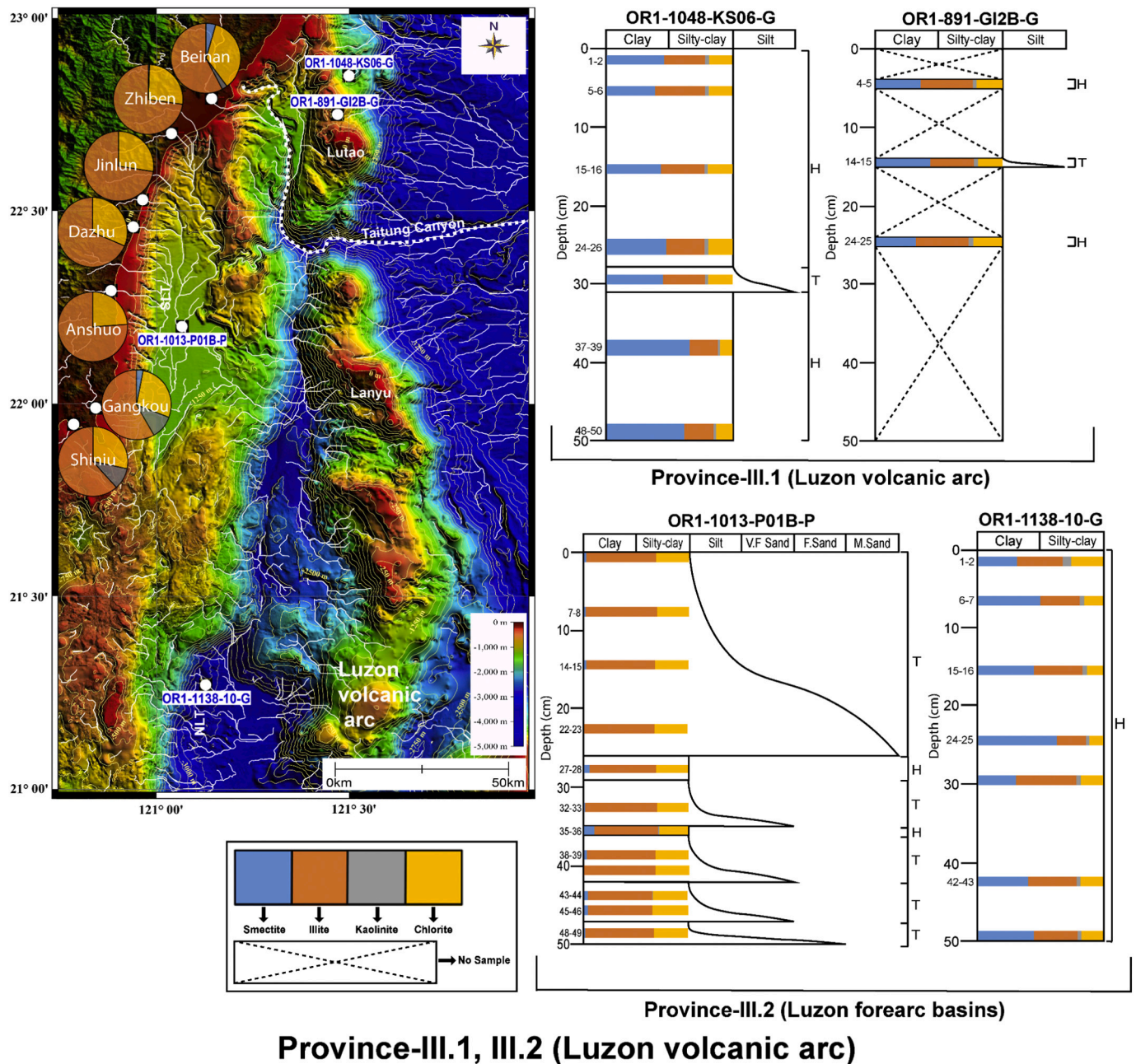
Fig. 8. Figure showing drainage patterns with distributions of clay mineral percentages in surrounding Taiwanese river sediments and lithological descriptions with vertical clay mineral distributions of the studied cores in Province: III.1, III.2. Abbreviations: NLT: North Luzon Trough, SLT: Southern Longitudinal Trough. *Contour lines* show the elevation in *250-m intervals*.

4.3. Distribution of clay minerals in different provinces

The clay mineral analysis in different provinces around Taiwan shows the spatial and downcore variations in the contents of clay minerals for both hemipelagites and turbidites of the studied sediment cores (Table S1, Figs. 6, 7, 8, 9, 10, 11). The ternary diagrams (Fig. 12a, b) of three end-member clay minerals of illite+chlorite, smectite, and kaolinite show that the clay-mineral assemblages in both hemipelagites and turbidites of different provinces change progressively between two end-members: illite+chlorite and smectite.

4.3.1. Ryukyu subduction zone (Province I)

The clay-mineral assemblages in both hemipelagites and turbidites in the sediment cores from western forearc basins consist mainly of illite

(48–60%) and moderate amounts of chlorite (20–44%) with no to small amounts of kaolinite (0–3%); besides, the amounts of smectite in hemipelagites are comparatively higher (9–26%) than turbidites (2–18%) (Province I.1; Fig. 6). Whereas, the hemipelagites and turbidites in the sediment cores from Hateruma forearc basin consist comparatively of more smectite (28–59%) and kaolinite (4–6%) (Province I.2; Fig. 6). Likewise, in the slope basins of the Yaeyama Ridge, the sediment core located to the south of the Hateruma Basin contain comparatively more smectite (27–57%) than the core located to the south of the Nanao Basin (16–36%) (Province I.3; Fig. 6).

4.3.2. Huatung Basin of the Philippine Sea Plate (Province II)

The sediment cores from levees of the Taitung Canyon consist only of turbidites and contain mainly illite (30–53%), comparatively less
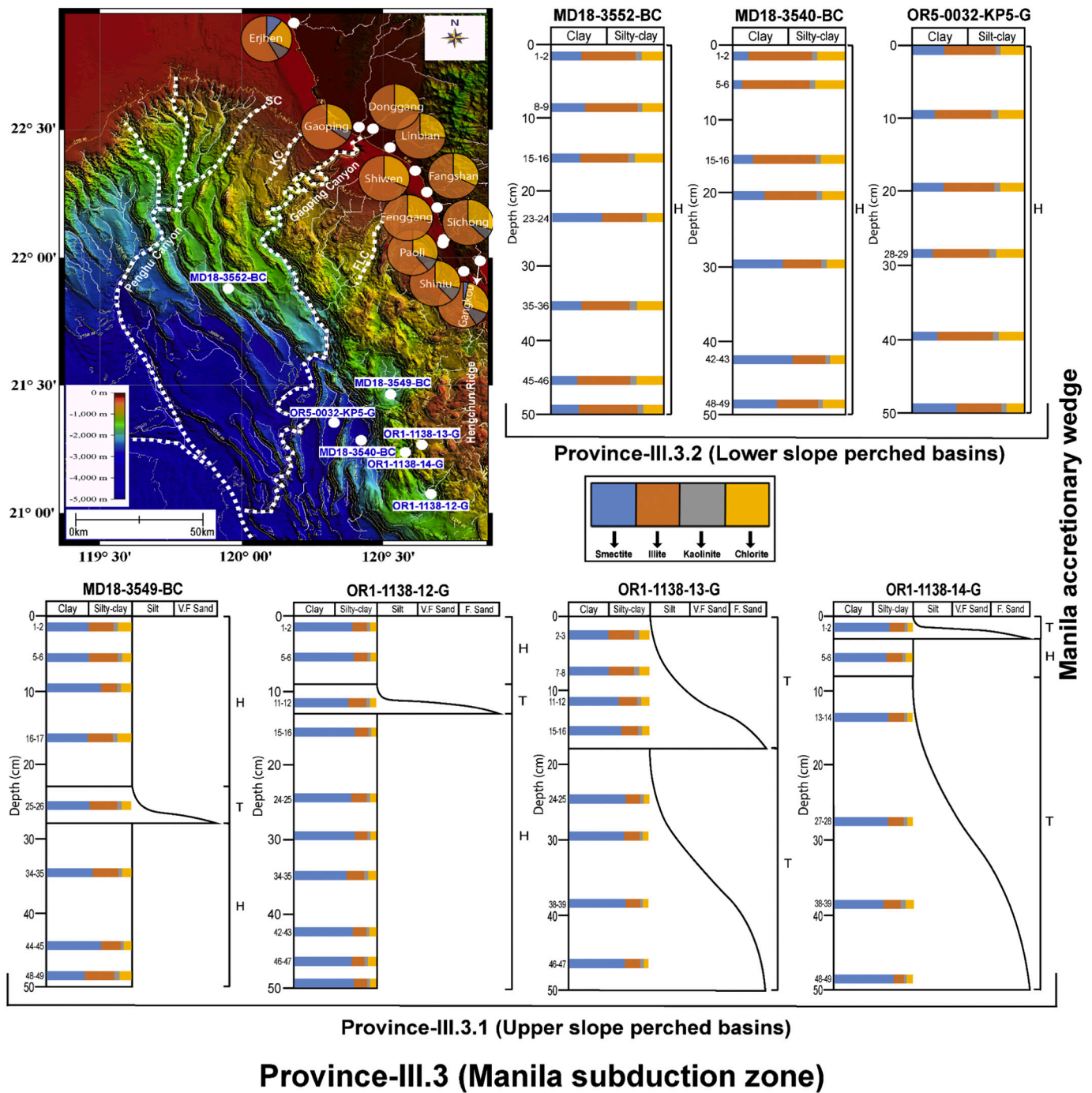
Fig. 9. Figure showing drainage patterns with distributions of clay mineral percentages in surrounding Taiwanese river sediments in Province III.3 and lithological descriptions with vertical clay mineral distributions of the studied cores in Provinces: III.3.1 and III.3.2. Abbreviations: FLC: Fangliao Canyon, KC: Kaohsiung Canyon, SC: Shousan Canyon. *Contour lines* show the elevation in *250- m intervals.*

smectite (17–49%), moderate amounts of chlorite (17–29%), and minor amounts of kaolinite (2–6%) (Province II.2; Fig. 7). Whereas, the core from a bathymetric high near the offshore Coastal Range of Taiwan consist only of hemipelagites and contain mainly smectite (41–66%), comparatively less illite (22–35%), moderate amounts of chlorite (11–22%), and scarce kaolinite (1–3%) (Province II.1; Fig. 7).

4.3.3. Manila subduction zone and the Luzon volcanic arc (Province III)

The clay-mineral assemblages in both hemipelagites and turbidites in the cores from the Luzon volcanic arc (located north of the Lutao Island), consist mainly of smectite (32–66%) and comparatively less illite

(23–42%) with moderate amounts of chlorite (10–22%) and scarce kaolinite (2–4%) (Province III.1; Fig. 8). Likewise, the hemipelagites in the core from the North Luzon Trough (NLT), an un-deformed Luzon forearc basin consist mainly of smectite (31–63%) and comparatively less illite (23–48%) (Province III.2; Fig. 8). Whereas, the hemipelagites and turbidites in the core from the Southern Longitudinal Trough (SLT), a deformed Luzon forearc basin adjacent to Taiwan, consist dominantly of illite (61–69%) and contain minor amounts of smectite (0–10%) (Province III.2; Fig. 8).

In the Manila accretionary wedge system (Province III.3), both hemipelagites and turbidites in the cores from the upper-slope perched
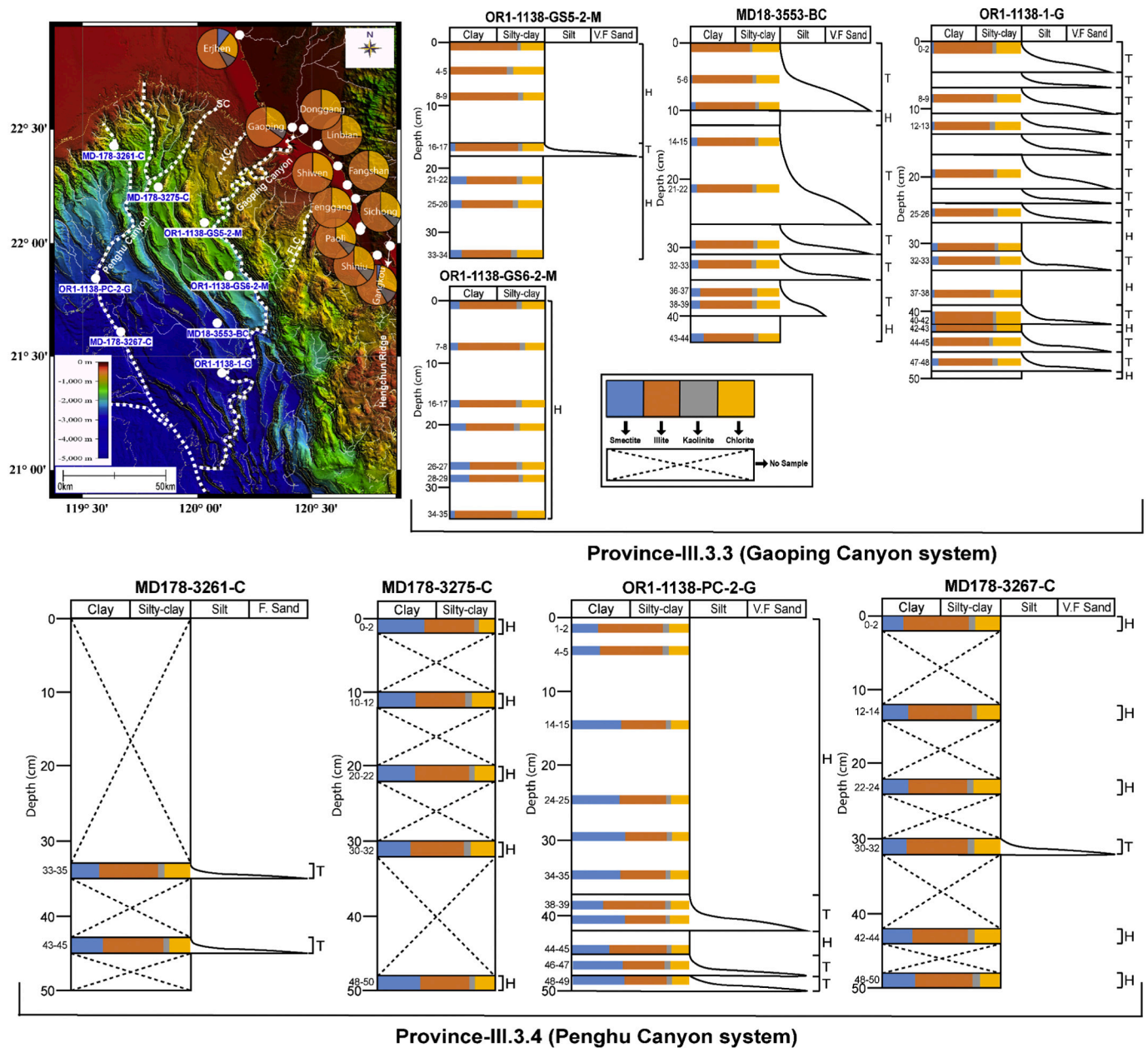
Fig. 10. Figure showing drainage patterns with distributions of clay mineral percentages in surrounding Taiwanese river sediments in Province III.3 and lithological descriptions with vertical clay mineral distributions of the studied cores in Provinces: III.3.3, III.3.4. Abbreviations: FLC: Fangliao Canyon, KC: Kaohsiung Canyon, SC: Shousan Canyon. *Contour lines* show the elevation in *250- m intervals*.

basins consist dominantly of smectite (45–75%) and contain moderate amounts of illite (13–35%) (Province III.3.1; Fig. 9). Whereas the cores from the lower-slope perched basins consist only of hemipelagites, consist mainly of illite (30–61%) and contain minor to high amounts of smectite (8–53%) (Province III.3.2; Fig. 9). The clay-mineral compositions in both hemipelagites and turbidites in the cores from the Gaoping and the Penghu Canyon systems (Provinces III.3.3, III.3.4; Fig. 10) are dominated by illite (50–72% and 35–56%, respectively) but with more smectite in the Penghu Canyon (18–45%) than in the Gaoping Canyon (0–20%).

4.3.4. NE South China Sea (Province IV)

In the NE South China Sea near Taiwan, the clay-mineral assemblages in both hemipelagites and turbidites in the sediment core from the lower Tainan continental slope consist mainly of smectite (49–57%) and comparatively less illite (29–35%) (Province IV.1; Fig. 11). In contrast, the core from middle Tainan continental slope consists mainly of Illite (35–47%) and comparatively less smectite (24–45%). The hemipelagites and turbidites in the sediment core from the middle reach of the Formosa Canyon consist mainly of smectite (30–61%) and contain comparatively less illite (26–46%). In contrast, the core from the distal part of Formosa Canyon located near the junction of the Penghu Canyon consists mainly of illite (40–68%) and contains scarce to moderate amounts of smectite (2–35%) (Province IV.2; Fig. 11).
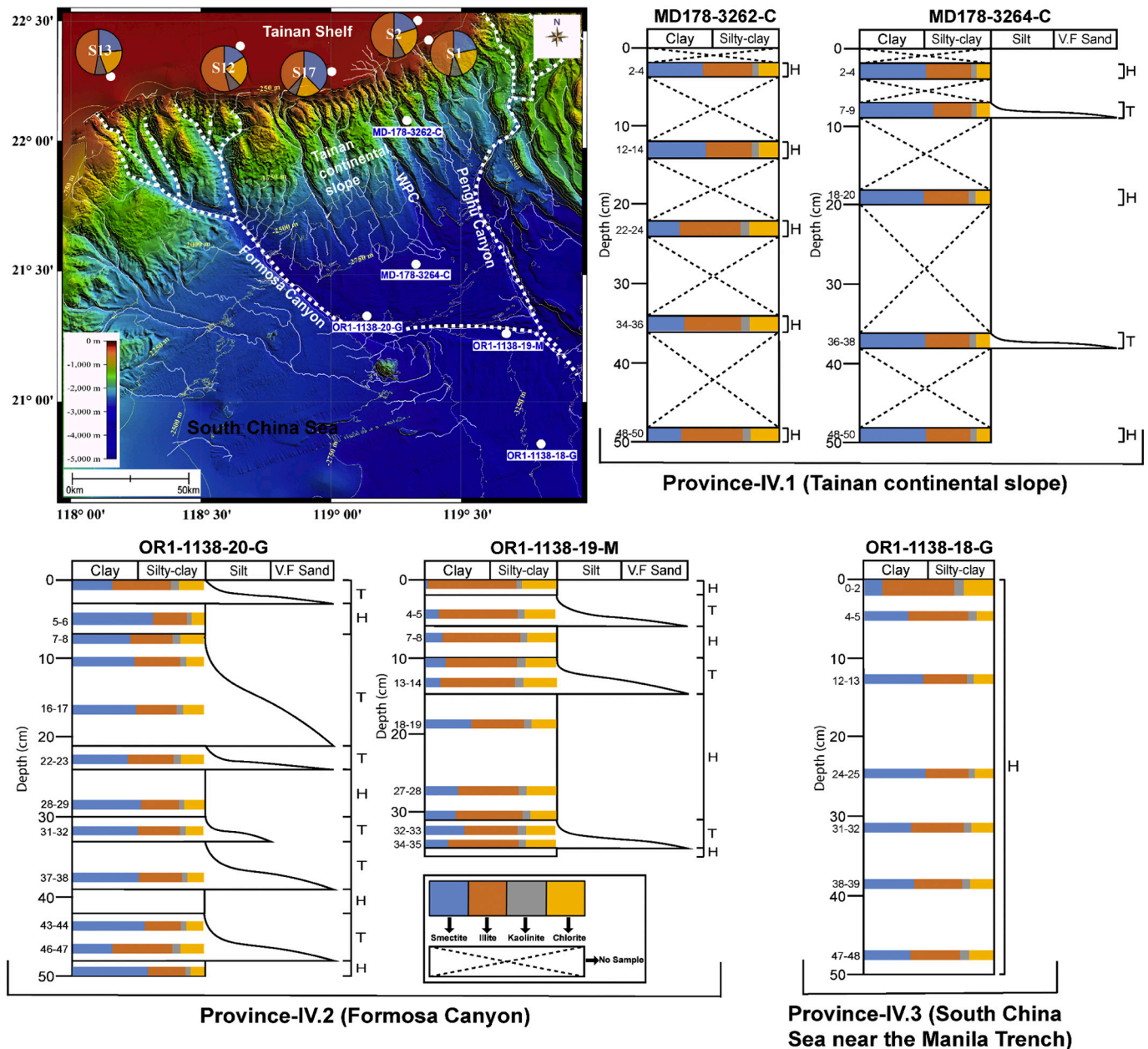
Fig. 11. Figure showing drainage patterns with distributions of clay mineral percentages in surrounding Taiwanese river sediments and lithological descriptions with vertical clay mineral distributions of the studied cores in Province-IV. Abbreviation: WPC: West Penghu Canyon. *Contour lines show the elevation in 250-m intervals.*

5. Discussion

5.1. Clay minerals at sediment sources

The main terrestrial sediment sources for the deep-sea areas around Taiwan are the Taiwan Island, the Luzon volcanic arc, Ryukyu Islands, and SE China. Prior studies pointed out that smectite is the characteristic clay mineral from Luzon Island and kaolinite is an index mineral from SE China, in particular from the Pearl River (Liu et al., 2007b; Liu et al., 2009; Liu et al., 2016b). As for the Ryukyu Islands, there is no literature reporting the characteristic clay minerals in river sediments. However, we expect that smectite would be the characteristic mineral for the Ryukyu Islands as their tectonic setting is similar to the Luzon Islands.

Our study shows that the clay minerals in river-mouth sediments around Taiwan consist mainly of illite (~60%) and chlorite (~30%)

with no or a small amount of kaolinite and smectite, except for some rivers in this study (see Section 4.2, Table S2). This indicates that illite and chlorite are the dominant clay minerals for Taiwan-derived sediments. The averaged contents of chlorite are relatively greater in eastern Taiwan (~33%) than in western Taiwan (~27%), in agreement with results by Li et al. (2011). Besides, we found that there is more smectite in river sediments sourced from the Coastal Range (see Section 4.2), suggesting that smectite is an additional characteristic clay mineral for sediments derived from eastern Taiwan, the Coastal Range in particular. The Coastal Ranged-derived smectite cannot be transported far away from the coast through hypopycnal sediment plumes as those river plumes will be diverted to the north and parallel to the coastline by the Kuroshio Current.

Comparing the clay-mineral compositions in Tainan Shelf sediments and southwest Taiwanese river-mouth sediments, we found that both
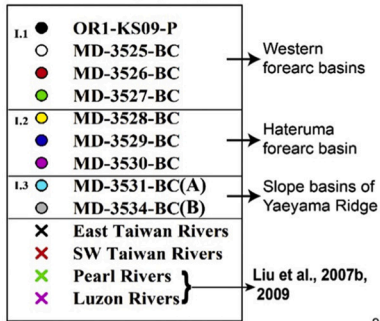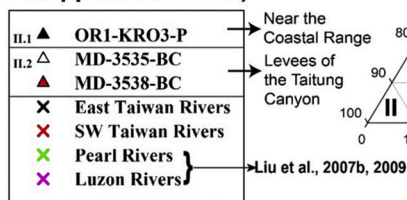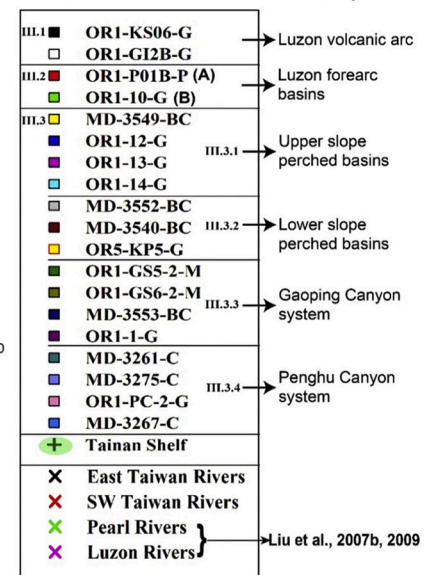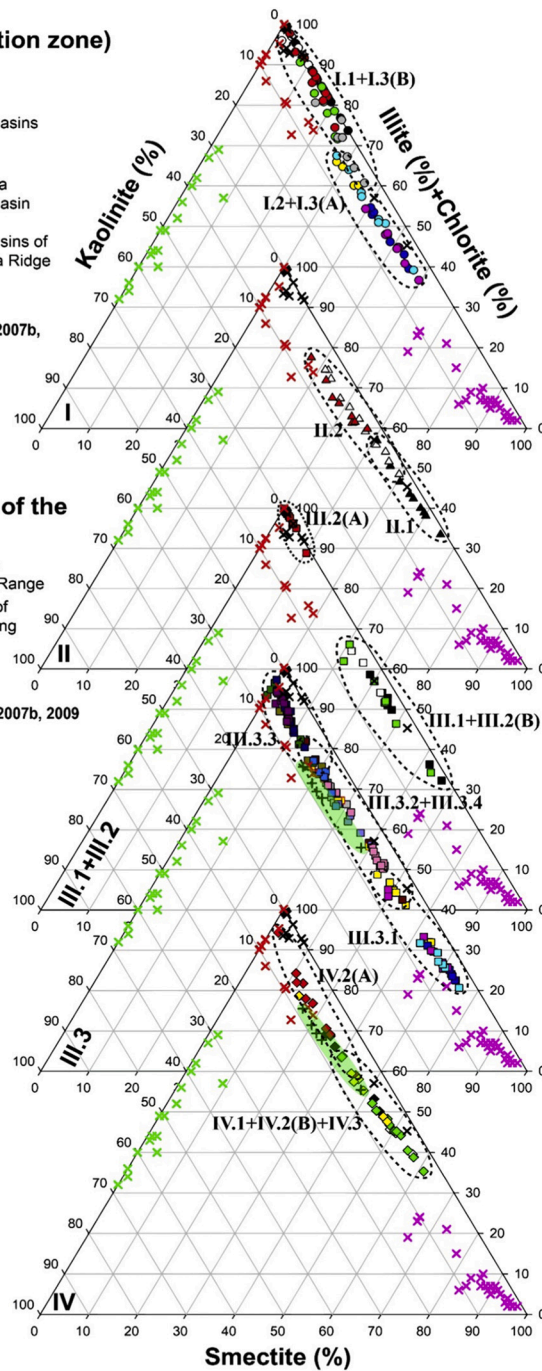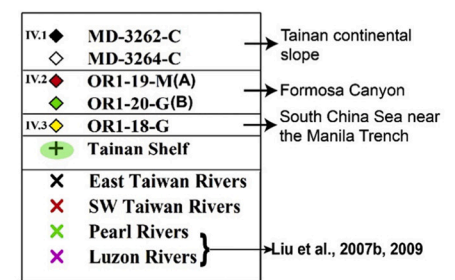
Fig. 12. (a) Comparison between clay mineral ternary diagrams of different provinces. (b) Ternary diagram of all provinces divided into turbidites and hemi-pelagites. Clay mineral data of Taiwan rivers and Tainan Shelf (this study), Pearl River (Liu et al., 2007b), and Luzon rivers (Liu et al., 2009) are plotted to track the source regions.

areas are dominated by illite but with more smectite and kaolinite in Tainan Shelf sediments than in southwest Taiwanese river-mouth sediments (see Section 4.2). Therefore, we consider the Tainan Shelf as one of the source domains. According to the literature and our study, we use three end-member clay minerals of illite+chlorite, smectite, and kaolinite to plot our results and to infer possible sediment sources (Fig. 12a, b). Also, we use the mineralogical ratio of smectite/(illite+chlorite) and kaolinite//(illite+chlorite) as an indicator of continental sources in order to reflect the source terranes (Fig. 13), and particularly the ratio smectite/(illite+chlorite) as an indicator of the Kuroshio

Current transport (e.g. Liu et al., 2010b).

5.2. Ages of studied sediment cores

We studied the top 50 cm of seafloor sediments to understand the sediment dispersal processes around Taiwan. The top 50 cm-thick seafloor sediments around Taiwan are generally deposited within a short period according to previous studies. For this short time span, the oceanic circulations, climate, and tectonics can be considered similar to the present-day situation. We expect high sedimentation rates in cores
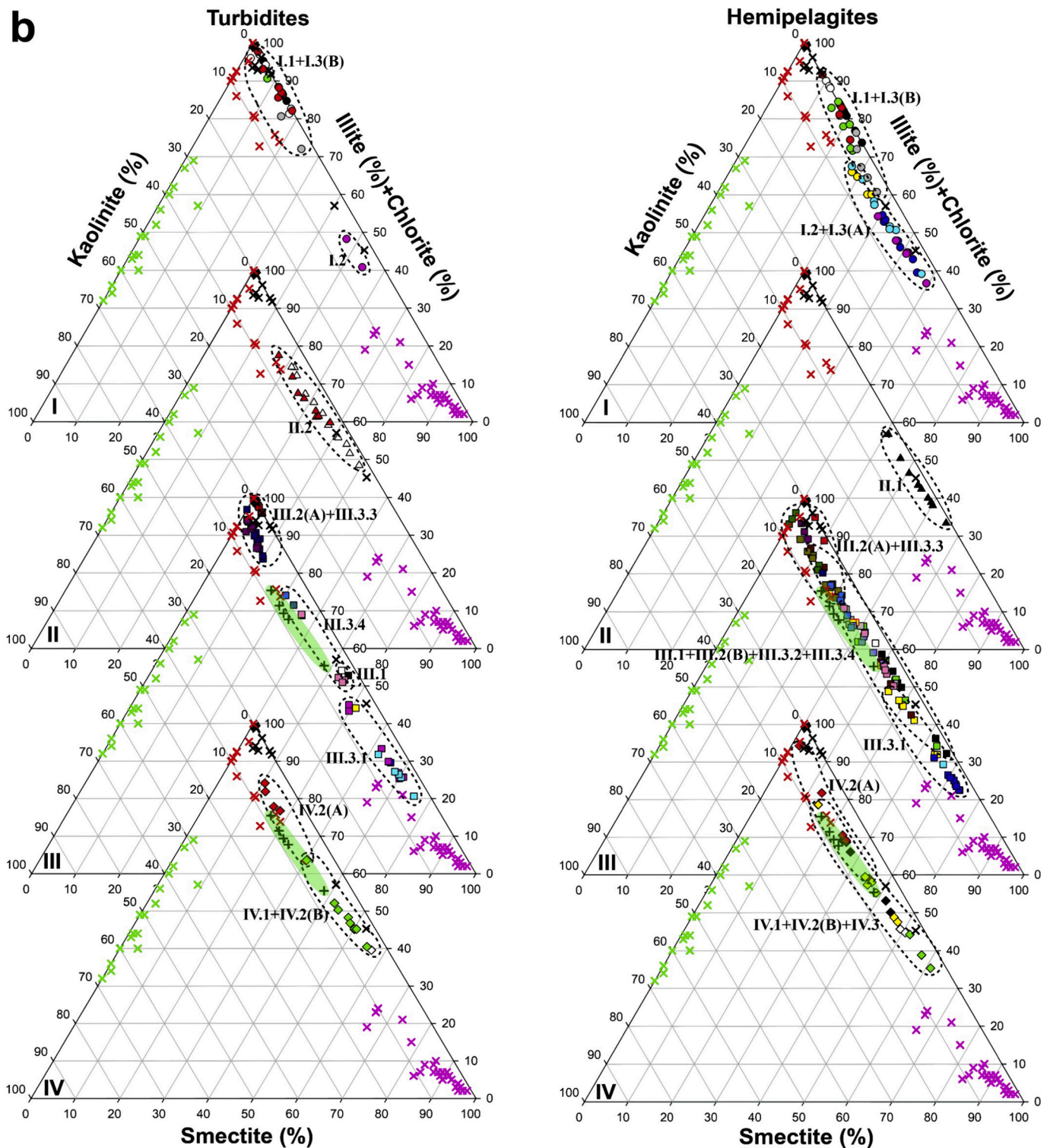
Fig. 12. (*continued*).

taken from locations along river-attached submarine canyon systems and areas close to land. For example, sedimentation rates along the Gaoping Canyon, range from up to 10 mm/yr in the canyon head (Huh et al., 2009) to 1.6 mm/yr in the middle of the canyon (Yu et al., 2017). In the upper slope and near the coastline of southwest Taiwan and away from the Gaoping Canyon, the rate of sedimentation is still high, up to 5 mm/yr (Wang et al., 2016; Su et al., 2018). From these studies, we assume high sedimentation rates in the river-connected Gaoping Canyon

system and for the upper slope close to the shoreline. Our studied cores (OR1-GS5–2-M, OR1-GS6–2-M, OR1–1-G, MD18–3553-BC) pertain to this category, indicating ages of the top 50 cm of these cores are typically less than 500 years.

Moderate to low sedimentation rates may be expected in the cores collected from sites in river-detached submarine canyon systems and in the perched basins without terrestrial sediment inputs. In the lower accretionary wedge lying in between the Penghu and Gaoping Canyon

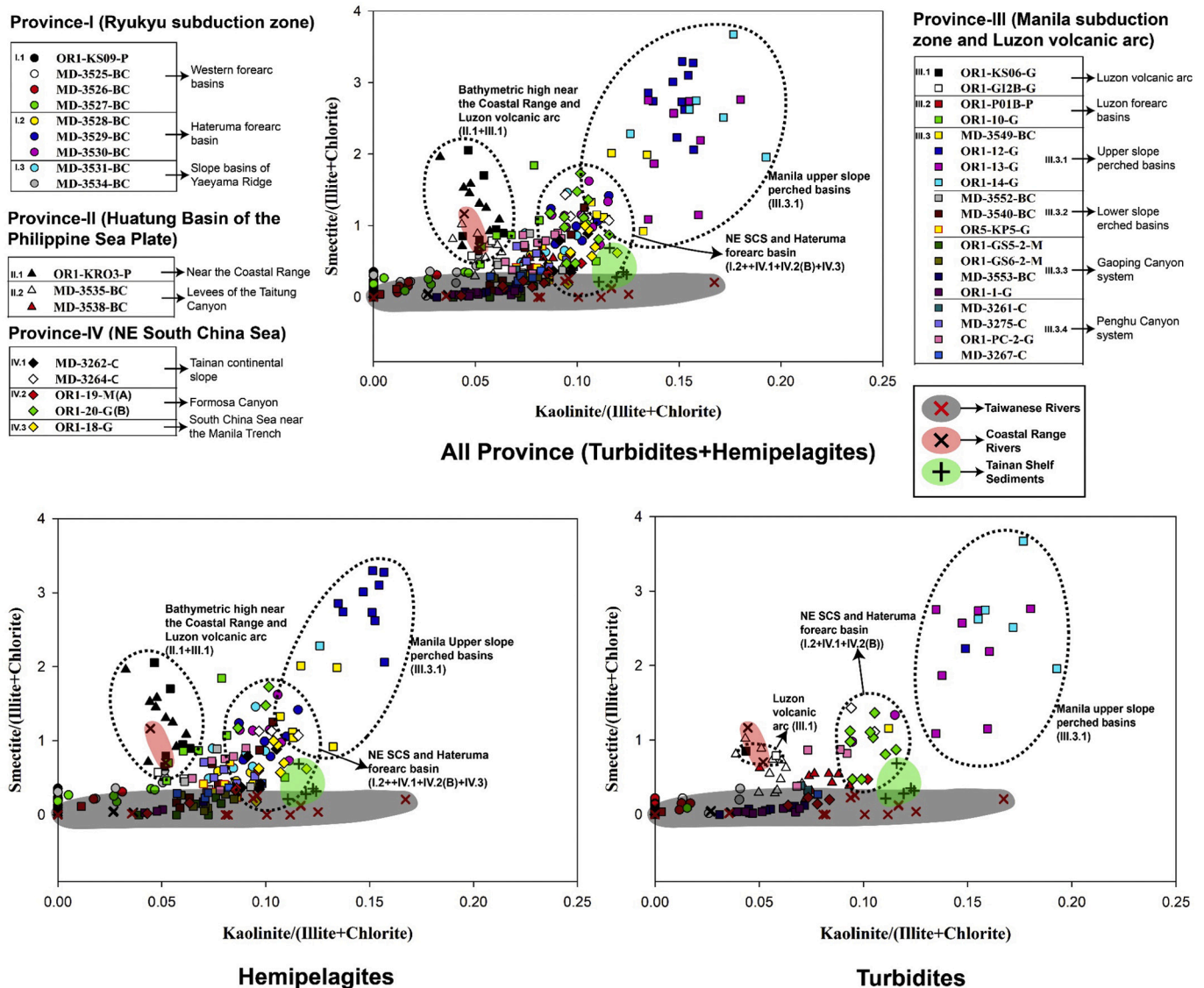**Fig. 13.** Binary diagrams showing smectite/(illite+chlorite) and kaolinite/(illite+chlorite) ratio for turbidites and hemipelagites of all provinces. Dashed lines indicate higher values of smectite/(illite+chlorite) and kaolinite/(illite+chlorite) ratios.

systems, the rate of sedimentation is still high as Lin et al. (2014) reported a rate of around 3 mm/yr at site MD05–2914 (water depth ∼ 1635 m). Therefore, we expect a relatively high sedimentation rate in our studied core located in the perched basin of the lower Manila accretionary wedge (MD18–3552-BC). As for the river-detached canyons, such as the Formosa Canyon, the rate of sedimentation is relatively low, up to ∼0.2 mm/yr as reported in Gong et al. (2012). So, for our studied cores along the Formosa Canyon (OR1–20-G, OR1–19-M), we believe low sedimentation rates, suggesting ages of the top 50 cm of the cores are typically less than ∼3000 years. Similarly, the Penghu Canyon is a river-detached canyon located closer to Taiwan, where we assume the rate of sedimentation should be slightly higher than that along the Formosa Canyon but less than that along the Gaoping Canyon. The top 50 cm sediments in the studied cores (OR1-PC2-G, MD178–3267-C, MD178–3275-C, MD178–3261-C) should also be less than ∼3000 years.

The lowest sedimentation rate is found in the areas without canyons/channels and far away from the shoreline. As pointed out by Su et al. (2018), the upper slope of the Manila accretionary wedge shows a relatively low sedimentation rate. Therefore, we assume a low sedimentation rate in the studied cores located in the upper-slope perched basins of the Manila accretionary wedge (OR-12-G, MD18–3549-BC,

OR1–14-G, OR1–13-G).

Similarly, in eastern Taiwan, we expect a high sedimentation rate for the cores in the river-connected submarine canyons such as in the levees of the Taitung Canyon (MD18–3535-BC and MD18–3538-BC). Whereas, the core P01B-P in the Southern Longitudinal Trough (SLT), is connected to the river-channel networks (Fig. 8), containing stacked turbidites indicating a high sedimentation rate. In the study by Lehu et al. (2016) and our study, we used two cores in common, those are OR1-KS06-G and OR1-KS09-P located in the slope of the Luzon volcanic arc and at the bottom of the slope of the Ryukyu arc near the Hoping Basin, respectively. In Lehu et al. (2016), it is estimated that the sedimentation rates for the mentioned cores are ∼1.05 mm/yr and ∼ 0.37 mm/yr, respectively, indicating a relatively lower sedimentation rate than the Gaoping Canyon system in southwest Taiwan. In addition, Lallemand et al. (2015) estimated the sedimentation rate for the studied core OR1-KR03-P, located offshore and near the Coastal Range on a bathymetric high, is up to ∼1.09 mm/yr for top 210 cm depth of sediments, suggesting a relatively high sedimentation rate.

The sedimentation rate in a few locations of our study area is not explored in previous studies. However, we believe that the cores in Nanao (MD18–3525-BC) and East Nanao (MD18–3526-BC and

MD18–3527-BC) basins that are not directly connected to the Hoping Canyon may have comparatively lower sedimentation rates than the cores collected from river-attached canyon systems. We also assume relatively low sedimentation rates for cores in the Hateruma forearc basin, which is located far away from Taiwan and not connected to any river-connected submarine canyons. Likewise, in southwest Taiwan, the cores from the Tainan continental slope (MD178–3262-C, MD178–3264-C) and in the South China Sea near the Manila Trench (OR1–18-G) are assumed to show relatively lower sedimentation rates than the cores located near land and connected to river-attached submarine canyons. Therefore, in our study, we assume the ages for the top 50 cm of the seafloor sediment cores located near Taiwan and river-connected submarine canyons around Taiwan are generally less than 500 years. Whereas, for the cores located in the river-detached submarine canyon system and in a few perched basins far away from Taiwan, the age may be up to ~3000 years.

5.3. Depositional mechanism of clay minerals for different sedimentary facies around Taiwan

5.3.1. Ryukyu subduction zone (Province I)

We divide the sedimentary units of the Ryukyu subduction zone into forearc basins and accretionary wedges with perched basins on top of folded-and-thrusted strata (Province-I; Fig. 1b). The forearc basins are separated by more or less north-trending bathymetric ridges (Fig. 6). The subdued bathymetric high between the Nanao and East Nanao Basins may impede most of the turbidity currents draining into the East Nanao Basin (MD18–3527-BC) as judged from much less turbidite occurrence in the East Nanao Basin (Fig. 6). The bathymetric ridge in between the East Nanao Basin and the Hateruma Basin is around 1500 m in height. This ridge becomes the barrier for eastward-directed turbidity currents flowing along the axis of a series of forearc basins in the study area.

The gravity-flow sediment deposition in the forearc basins of the Hoping, Nanao, and East Nanao basins (Province-I.1; Fig. 6) is primarily caused by downslope transport of sediments from the Taiwan Island, Ryukyu arc massif, and the Yaeyama accretionary prism (e.g., Hsiung et al., 2017; Lallemand et al., 2013; Lehu et al., 2015). A few channels on the western slope of the Hoping Basin serve as major conduits for coarse sediments delivered from Taiwanese rivers (i.e., Dongaobei, Heping, and Nanao rivers) to the Hoping and Nanao Basins through the Heping Canyon system (Fig. 6). This indicates that flood-induced hyperpycnal turbidity currents should also be an important agent for transporting Taiwan-derived sediments into the forearc basins. Our clay mineral study also suggests similar sedimentary processes for the deposition of turbidites as judged from high amounts of illite and chlorite in the silty and sandy turbidites of the sediment cores from western forearc basins (see Section 4.3.1, Fig. 6). Besides, the hemipelgites in the sediment

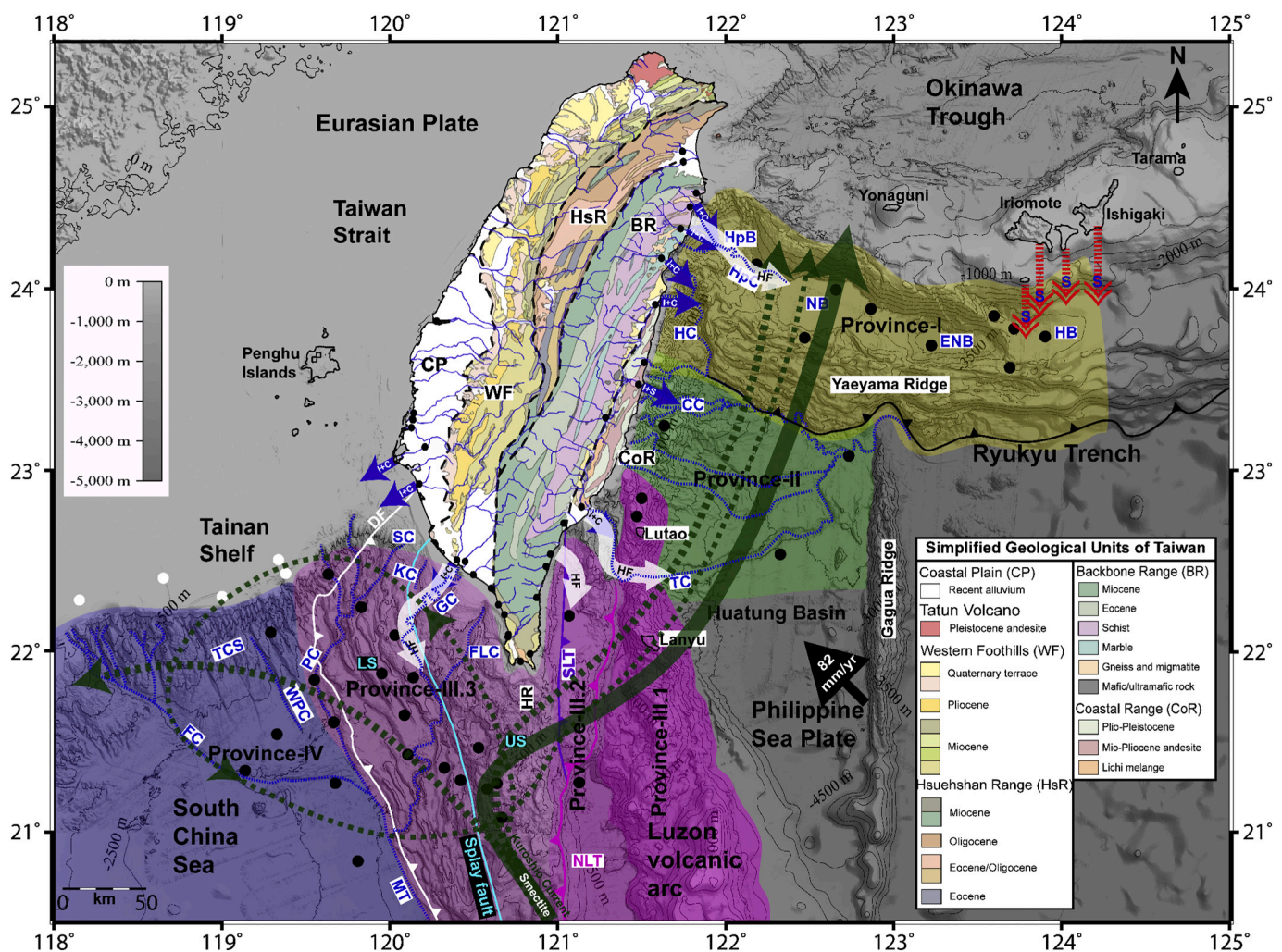**Fig. 14.** Map showing a synopsis of spatial sediment transport processes/paths in the deep seas around Taiwan based on characteristic clay minerals from various source terrains. The arrows in black (solid and dashed) showing the different types of Kuroshio intrusion (modified from Caruso et al., 2006). Abbreviations: HF: Hyperpycnal flows, I: Illite, C: Chlorite, S: Smectite. See Fig. 1 for other abbreviations.

cores from western forearc basins and perched slope basins of the Yaeyama accretionary wedge, south to the Nanao Basin (MD18–3534-BC), contain higher amounts of smectite than the turbidites (see Section 4.3.1, Fig. 6), indicating that the Kuroshio Current pathways may contribute minor to moderate amounts of smectite to the sites.

The gravity-flow deposition in the Hateruma forearc basin (Province-I.2; Fig. 6) can be caused by downslope transport of sediments from the nearby Ryukyu arc massif and islands (i.e., Yonaguni, Iriomote, Ishigaki, Tarama islands), and the Yaeyama accretionary prism. The amount of smectite and kaolinite in the Hateruma forearc basin is higher than in western forearc basins (see Section 4.3.1, Fig. 6). This indicates that smectite from the Ryukyu Islands may have been transported to the Hateruma forearc basin (Fig. 14). As well, the high amounts of smectite in the perched slope basins located to the south of the Hateruma Basin (MD18–3531-BC), also indicates that the Ryukyu Islands are additional clay mineral sources to this site.

The source for kaolinite in the Hateruma Basin is unclear. A study of the ODP1202B core (Diekmann et al., 2008), located in the Southern Okinawa Trough near Taiwan, shows around ~7% of kaolinite for recent sediments. Diekmann et al. (2008) and Dou et al. (2010) interpreted the source of kaolinite as most likely derived from the East China Sea shelf. We, therefore, assume that the source of kaolinite in the Hateruma Basin is also most likely from the East China Sea shelf.

5.3.2. Huatung Basin of the Philippine Sea Plate (Province II)

The Huatung Basin lies offshore from eastern Taiwan and is bounded by the Ryukyu Trench in the north, the Gagua Ridge in the east, and the Luzon arc in the west (Fig. 1b). Three river-connected submarine canyons influence the northern Huatung Basin near Taiwan: the Hualien Canyon, the Chimei Canyon, and the Taitung Canyon from north to south, reaching into the river mouths of the Hualien, Xiuguluan, and Beinan rivers, respectively (Fig. 1b). They receive sediments discharged from the Central Range and the Coastal Range of Taiwan to the Huatung Basin (Lehu et al., 2015; Malavieille et al., 2002). Frequent occurrences of turbidity currents (Lehu et al., 2015) along the above three river-connected canyon systems indicate that flood-induced hyperpycnal turbidity currents may be an important agent for transporting Taiwan-derived sediments into the Huatung Basin.

This study examined sediments recovered from levees of the Taitung Canyon at two sites of MD18–3535-BC and MD18–3538-BC, as well as at one site, OR1-KR03-P, located in an isolated bathymetric high south of the Chimei Canyon (Fig. 7). The very fine-grained sandy and silty turbidites on levees of the Taitung Canyon consist mainly of illite and smectite (see Section 4.3.2, Fig. 7). These turbidites are interpreted to result from overspilling of flood-induced turbidity currents from the Taitung Canyon or the Hualien Canyon and its tributary (the Chimei Canyon), carrying sediments sourced from eastern Taiwan (Coastal Range and Central Range; Fig. 2) and the Luzon volcanic arc.

The core on the bathymetric high near the Coastal Range of Taiwan is not affected by turbidity currents and contains only hemipelagic deposits (Fig. 7). They consist mainly of smectite and comparatively less illite (see Section 4.3.2, Fig. 7), indicating that the main clay mineral source for this site is from Luzon through the Kuroshio Current flow path with additional contribution from the Coastal Range of Taiwan.

5.3.3. Manila subduction zone and the Luzon volcanic arc (Province III)

We divide the Manila subduction zone and the Luzon volcanic arc off southern Taiwan into morphotectonic units of the North Luzon volcanic arc, Luzon forearc basins, and the Manila accretionary wedge from east to west (Fig. 1b). The Luzon forearc basins can be sub-divided into the North Luzon Trough (NLT), an undeformed forearc basin, and the Southern Longitudinal Trough (SLT), a deformed forearc basin near the Taiwan orogen. The Manila accretionary wedge, lying in between the Manila Trench to the west and the NLT to the east, can be sub-divided into the lower-slope and upper-slope domains by the splay fault. The western part of the accretionary wedge is influenced by two major

canyon systems, namely the Penghu and Gaoping canyons draining sediments from the Taiwan orogen (Fig. 1b).

The sediment cores in the colliding Luzon volcanic arc, north of the Lutao Island are completely disconnected from any major river drainage systems and are mainly consist of smectite and illite (see Section 4.3.3, Fig. 8). This indicates the thin silty turbidites in this location were most likely triggered by the slope failure of sediments from the Luzon volcanic arc, and the hemipelagites can be sourced from the Luzon volcanic arc, the Lutao Island, and Taiwan.

The sediment core from the SLT contains multiple layers of very fine to medium-grained sandy turbidites (Fig. 8), indicating dominantly turbidite deposition in the locale (Lehu et al., 2015). The turbidites and hemipelagites in this core consist dominantly of illite with moderate chlorite (see Section 4.3.3, Fig. 8), indicating that the sediment source is predominantly from Taiwan. There are many submarine channels in the SLT, with channel heads connecting to rivers, such as the Zhiben River, the Jinlun River, and the Dazhu River in southeast Taiwan (Fig. 8) serve as major conduits for coarse sediments delivering from Taiwanese rivers. This indicates that flood-induced hyperpycnal turbidity currents and hypopycnal plumes off river mouths are major agents for transporting Taiwan-derived sediments into the SLT. However, the sediment core from the NLT consists only of hemipelagites and contains mainly of smectite with comparatively less illite (see Section 4.3.3, Fig. 8), indicates that hemipelagites are sourced from the Luzon volcanic arc through the Kuroshio Current and Taiwan.

In the upper-slope perched basins of the Manila accretionary wedge, the hemipelagites and sandy turbidites in the sediment cores consist predominantly of smectite (Fig. 9). This indicates that higher amounts of smectite have been delivered from Luzon into the Hengchun Ridge through strong Kuroshio Current effects, and these sandy turbidities are derived by slope failure in the submarine Hengchun Ridge.

In the lower-slope domain and along the river-connected Gaoping Canyon, the sediment cores from the west bank (OR1–1-G) and Slope fan (MD18–3553-BC; Hsiung et al., 2018) of the lower Gaoping Canyon contain frequent, very fine-grained sandy turbidites (Fig. 10), indicating the coring sites are highly influenced by overspilling of turbidity currents from the Canyon. In contrast, the sediment cores from the west bank of the upper Gaoping Canyon (OR1-GS5–2-M and OR1-GS6–2-M) consist dominantly of hemipelagites (Fig. 10). This may be due to the coring sites being located with an elevation of around 500 m above the adjacent canyon thalweg, restricting the influence of overspilling turbidity currents from the canyon. Both the hemipelagites and turbidites in the sediment cores consist mainly of illite and chlorite (see Section 4.3.3, Fig. 10). This suggests the flood-induced hyperpycnal turbidity currents and hypopycnal plumes off river mouths are major agents for transporting Taiwan-derived sediments into the Gaoping Canyon system. Moreover, the hemipelagites and turbidites in the sediment cores from the Penghu Canyon system consist mainly of illite with moderate to high amounts of smectite (see Section 4.3.3, Fig. 10). This suggests that hemipelagites are sourced mainly from Taiwan, and Luzon through the Kuroshio Current, while turbidites are derived by overspilling turbidity currents from the canyon.

The amount of smectite in the Penghu Canyon system is higher than in the Gaoping Canyon system, indicating that the Gaoping Canyon is dominantly influenced by the river-canyon system, diluting the smectite supplied through the Kuroshio Current. According to Zhang et al. (2018), the hyperpycnal flows associated with river floods during typhoons are the main triggering mechanism for transportation of terrestrial sediments into the deep sea in the river canyon system like the Gaoping Canyon system. Therefore, the clay mineral compositions of the sediment cores along the Gaoping Canyon system are similar to that of the Gaoping River (Fig. 10, Tables S1, S2).

The sediment cores in the perched basins of the Manila lower-slope domain and south of the Gaoping Canyon consist mainly of illite (30–61%) and contain minor to high amounts of smectite (8–53%) (Fig. 9), indicating that the clay minerals can be sourced from Luzon

through the Kuroshio Current and overspilling of sediments from the Gaoping Canyon. The variations in smectite amounts in the Manila accretionary wedge system such as from high to moderate in the upper-slope perched basins and Penghu Canyon system, respectively, show the strength of the Kuroshio Current.

5.3.4. NE South China Sea (Province IV)

We divide the NE South China Sea near Taiwan into depositional units of the Tainan continental slope (TCS), Formosa Canyon, and SCS near the Manila Trench, which is located south of the Gaoping and Penghu Canyon systems (Fig. 1b). The variations in smectite amounts such as higher in the lower TCS than the upper TCS and Tainan Shelf sediments (see Sections 4.2 and 4.3.4, Fig. 11), indicate that the strength of the Kuroshio Current decreases along the Tainan Shelf boundary.

The presence of more smectite and comparatively less illite in the middle reach of the Formosa Canyon (OR1–20-G) (see Section 4.3.4, Fig. 11), suggests that the clay mineral sources of hemipelagites are mainly derived from Luzon through the Kuroshio Current and secondarily from Taiwan, and turbidites may have been caused by slope failures in the Formosa Canyon. In contrast, the presence of more illite and chlorite in the distal part of the Formosa Canyon and near the confluence of the Penghu Canyon (OR1–19-M; Fig. 11), indicates the influence of overspilled turbidity currents from the Penghu Canyon, providing Taiwan-derived sediments to the Formosa Canyon.

The relatively high kaolinite content in the TCS and the middle reach of the Formosa Canyon (Fig. 13) indicate that Tainan Shelf sediments have been one of the source contributors for TCS and Formosa Canyon as judged from the presence of more kaolinite in Tainan shelf sediments. The sediment core from the South China Sea near the Manila Trench consists mainly of illite and smectite (Fig. 11), indicating that the clay minerals are sourced from Taiwan and Luzon.

5.4. Summary of source and transport mechanism of clay minerals around Taiwan

As discussed above, we assume that the top 50 cm of studied cores around Taiwan are recent sediments (≤ 3000 yr B·P) and for this short time span, the oceanic circulations, climate, and tectonics can be considered similar to the present-day situation. From our clay mineral results, it is clear that the clay mineral assemblages in the studied cores around Taiwan are mainly controlled by supply from major provenance via current transport. The clay-mineral assemblages in both hemipelagites and turbidites of different provinces change progressively between two end-members: illite+chlorite and smectite (Fig. 12b). Illite and chlorite are derived predominantly from Taiwan river sediments and smectite is derived predominantly from Luzon river sediments. Scarce to minor amounts of kaolinite in the studied sediments indicate no contributions of sediments from rivers in SE China (Fig. 12a).

The spatial and downcore variations of clay mineral contents in hemipelagites of the studied sediment cores indicate that the hemipelagic sediments are derived from various provenances, and transported through the Kuroshio Current and other oceanic currents or hypopycnal plumes off river mouths, which encompasses a wide geographic area (Fig. 14). The minor to significant downcore variations in the studied cores mainly depends on the varying strength of surface currents and types of transport (e.g., cyclonic circulations, Caruso et al., 2006, and seasonal changes of paths for the Kuroshio Current, Nan et al., 2015).

The spatial variation of clay mineral contents in turbidites from different provinces depends on the various sources and depositional processes involved in individual provinces, such as slope failures, channelized turbidity currents, and overspilling of turbidity currents from canyons. The downcore variation of clay-mineral contents can be seen among the turbidites (from 4% to 28%). or within a turbidite (from 1% to 25%) of studied sediment cores. This changing clay-mineral content among turbidites in a core probably reflects different sediment sources. Whereas the changing clay-mineral content within a turbidite is a bit complicated. We do not notice any systematic shift in clay-mineral contents within a turbidite. The variation is evident for the coarse turbidite fraction only in a few turbidites with less smectite in the coarse fraction of the turbidite compared to the finer fraction of the turbidite and hemipelagites (e.g., core MD18–3525-BC and MD18–3526-BC in Fig. 6 and Fig. S1). This changing clay-mineral content within a fining-upward turbidite is probably due to different depositional agents. The coarse fractions are predominantly tractional deposits from the turbidity current itself, whereas the finer sediments mainly accumulated from suspension clouds related to turbidity currents or from other sediment sources such as nepheloid layers (e.g., Baker, 1976). Therefore, in the cores MD18–3525-BC and MD18–3526-BC, the coarse fraction of the turbidites consist dominantly of illite and chlorite and contain scarce amounts of smectite, indicating more influence of tractional deposits from the turbidity currents derived from Taiwanese rivers. In most of the studied cores, the relative abundance of clay minerals within turbidites and hemipelagites is quite similar. Therefore, we argue that the adjacent turbidites and hemipelagites of a core share common detrital clay sources.

Assuming that there is no illite formed by diagenesis and it is of detrital origin in studied sediment samples, we use illite chemistry index and illite crystallinity as indicators of the intensity of chemical weathering. The values of illite chemistry index and illite crystallinity for the studied sediment samples are <0.5 and ≤ 0.45 (°Δ2θ), respectively (Table S1). They both imply Fe-Mg rich un-weathered illite, characteristic of physically eroded rocks (Kuo et al., 2012; Liu et al., 2007b; Wan et al., 2010).

High ratios of smectite/(illite+chlorite) in the cores from a bathymetric high off the Coastal Range, the Luzon volcanic arc, the upper-slope perched basins of the Manila accretionary wedge, and few cores in the northeast South China Sea off southwestern Taiwan (Fig. 13) consist dominantly of smectite, indicating strong influence by Kuroshio Current pathways that bring smectite from the Luzon (Fig. 14). The high ratio of kaolinite/(illite+chlorite) in the upper-slope perched basins (Fig. 13) indicates that the kaolinite may derive locally from the Hengchun Peninsula, as the river-mouth sediments from the Gangkou, Paoli, and Shiniu rivers in the Hengchun Peninsula contain more kaolinite (~8–11%). The moderate ratio of kaolinite/(illite+chlorite) in the Tainan continental slope and middle part of the Formosa Canyon (OR1–20-G) indicate that the kaolinite may derive from Tainan Shelf sediments (Fig. 13). The Hoping Canyon, the Nanao Basins, the Southern Longitudinal Trough off eastern Taiwan, and the Gaoping Canyon off southwest Taiwan consist dominantly of illite and chlorite, interpreted as derived mainly from Taiwanese rivers by the river-fed hyperpycnal and hypopycnal flows (Fig. 14).

6. Conclusions

For the first time, we studied the clay mineralogy of recent deep-sea sediments around Taiwan in hemipelagites and turbidites within the top 50 cm of the sediment cores to determine the source and transport of detrital fine-grained sediments. River-mouth sediments around Taiwan were also studied for clay mineralogy to constrain the source characteristics of the Taiwanese rivers. Our results show that the clay mineral assemblages in both hemipelagites and turbidites of different provinces progressively change between two major end-members: illite+chlorite and smectite. Illite and chlorite are sourced from Taiwan whereas smectite is mainly transported from Luzon by the Kuroshio Current. However, smectite can also be sourced from the Coastal Range of Taiwan and the Ryukyu Islands. In summary, we propose that the sediment cores consisting dominantly of illite and chlorite are associated mainly with river-related canyon systems, interpreted as derived mainly from Taiwanese rivers by hyperpycnal and hypopycnal flows, whereas the sediment cores consisting dominantly of smectite, indicating strong influence by Kuroshio Current pathways. The relative abundances of

clay minerals in the adjacent turbidites and hemipelagites are quite similar, indicating that they share common detrital clay sources, but the variation of clay minerals is more evident in a few coarse turbidite fractions. Our study of clay mineralogy and sediment provenances for recent deep-water seafloor sediments around Taiwan can serve as a reference for paleoclimatic and paleoceanographic reconstructions around Taiwan.

Declaration of Competing Interest

The authors declare that they have no known competing financial interests or personal relationships that could have appeared to influence the work reported in this paper.

Acknowledgements

Appendix A. Supplementary data

Supplementary data to this article can be found online at https://doi.org/10.1016/j.tecto.2021.228974.

References

Baker, E.T., 1976. Distribution, composition, and transport of suspended particulate matter in the vicinity of Willapa submarine canyon, Washington. GSA Bull. 87, 625–632.

Biscaye, P.E., 1965. Mineralogy and sedimentation of recent deep-sea clay in the Atlantic Ocean and adjacent seas and oceans. GSA Bull. 76, 803–832.

Burbank, D.W., Blythe, A.E., Putkonen, J., Pratt-Sitaula, B., Gabet, E., Oskin, M., Barros, A., Ojha, T.P., 2003. Decoupling of erosion and precipitation in the Himalayas. Nature 426, 652–655.

Canfield, D.E., 1997. The geochemistry of river particulates from the continental USA: Major elements. Geochim. Cosmochim. Acta 61, 3349–3365.

Caruso, M.J., Gawarkiewicz, G.G., Beardsley, R.C., 2006. Interannual variability of the Kuroshio intrusion in the South China Sea. J. Oceanogr. 62, 559–575.

Chen, C.H., 2000. Geologic Map of Taiwan, Scale 1:500.000.

Clift, P., Carter, A., Campbell, I., Pringle, M., Lap, N., Allen, C.M., Hodges, K., Tan, M., 2006. Thermochronology of mineral grains in the Red and Mekong Rivers, Vietnam: Provenance and exhumation implications for Southeast Asia. Geochem. Geophys. Geosyst. 7.

Dadson, S.J., Hovius, N., Chen, H., Dade, W.B., Hsieh, M.L., Willett, S.D., Hu, J.C., Horng, M.J., Chen, M.C., Stark, C.P., Lague, D., Lin, J.C., 2003. Links between erosion, runoff variability and seismicity in the Taiwan orogen. Nature 426, 648–651.

Diekmann, B., Wopfner, H., 1996. Petrographic and diagenetic signatures of climatic change in peri- and postglacial Karoo Sediments of SW Tanzania. Palaeogeogr. Palaeoclimatol. Palaeoecol. 125, 5–25.

Diekmann, B., Hofmann, J., Henrich, R., Fütterer, D.K., Röhl, U., Wei, K.-Y., 2008. Detrital sediment supply in the southern Okinawa Trough and its relation to sea-level and Kuroshio dynamics during the late Quaternary. Mar. Geol. 255, 83–95.

Dou, Y., Yang, S., Liu, Z., Clift, P.D., Yu, H., Berne, S., Shi, X., 2010. Clay mineral evolution in the Central Okinawa Trough since 28ka: Implications for sediment provenance and paleoenvironmental change. Palaeogeogr. Palaeoclimatol. Palaeoecol. 288, 108–117.

Gaillardet, J., Dupré, B., Louvat, P., Allègre, C.J., 1999. Global silicate weathering and CO2 consumption rates deduced from the chemistry of large rivers. Chem. Geol. 159, 3–30.

Gingele, F.X., 1996. Holocene climatic optimum in Southwest Africa—evidence from the marine clay mineral record. Palaeogeogr. Palaeoclimatol. Palaeoecol. 122, 77–87.

Gingele, F., Deckker, P., Hillenbrand, C.-D., 2001. Clay mineral distribution in surface sediments between Indonesia and NW Australia - source and transport by ocean currents. Mar. Geol. 179, 135–146.

Gong, C., Wang, Y., Peng, X., Li, W., Qiu, Y., Xu, S., 2012. Sediment waves on the South China Sea Slope off southwestern Taiwan: implications for the intrusion of the Northern Pacific Deep Water into the South China Sea. Mar. Pet. Geol. 32, 95–109.

Holtzapffel, T., 1985. Les Minéraux Argileux: Préparation, Analyse Diffractométrique et Determination, 12. Soc. Géol. Nord Publ (136 pp).

Hsieh, Y.-H., Liu, C.-S., Suppe, J., Byrne, T.B., Lallemand, S., 2020. The chimei submarine canyon and fan: a record of Taiwan arc-continent collision on the rapidly deforming overriding plate. Tectonics 39 (e2020TC006148).

Hsiung, K.-H., Kanamatsu, T., Ikehara, K., Shiraishi, K., Horng, C.-S., Usami, K., 2017. Morpho-sedimentary features and sediment dispersal systems of the southwest end of the Ryukyu Trench: a source-to-sink approach. Geo-Mar. Lett. 37, 561–577.

Hsiung, K.-H., Yu, H.-S., Chiang, C.-S., 2018. The modern Kaoping transient fan offshore SW Taiwan: Morphotectonics and development. Geomorphology 300, 151–163.

Huang, J., Wan, S., Xiong, Z., Zhao, D., Liu, X., Li, A., Li, T., 2016. Geochemical records of Taiwan-sourced sediments in the South China Sea linked to Holocene climate changes. Palaeogeogr. Palaeoclimatol. Palaeoecol. 441, 871–881.

Huh, C.-A., Lin, H.-L., Lin, S., Huang, Y.-W., 2009. Modern accumulation rates and a budget of sediment off the Gaoping (Kaoping) river, SW Taiwan: a tidal and flood dominated depositional environment around a submarine canyon. J. Mar. Syst. 76, 405–416.

Kaifu, Y., Kuo, T.-H., Kubota, Y., Jan, S., 2020. Palaeolithic voyage for invisible islands beyond the horizon. Sci. Rep. 10, 19785.

Kandasamy, S., Chen, C.-T.A., 2006. Moderate chemical weathering of subtropical Taiwan: constraints from solidphase geochemistry of sediments and sedimentary rocks. J. Geol. 114, 101–116.

Kao, S.-J.I., Milliman, J., 2008. Water and sediment discharge from small mountainous Rivers, Taiwan: the roles of lithology, episodic events, and human activities. J. Geol. 116, 431–448.

Kuo, L.-W., Song, S.-R., Yeh, E.-C., Chen, H.-F., Si, J., 2012. Clay mineralogy and geochemistry investigations in the host rocks of the Chelungpu fault, Taiwan: Implication for faulting mechanism. J. Asian Earth Sci. 59, 208–218.

Lallemand, S., Theunissen, T., Schnürle, P., Lee, C.-S., Liu, C.-S., Font, Y., 2013. Indentation of the Philippine Sea plate by the Eurasia plate in Taiwan: details from recent marine seismological experiments. Tectonophysics 594, 60–79.

Lallemand, S., Lehu, R., Rétif, F., Hsu, S.-K., Babonneau, N., Ratzov, G., Bassetti, M.-A., Dezileau, L., Hsieh, M.-L., Dominguez, S., 2015. A ~3000 years-old sequence of extreme events revealed by marine and shore deposits east of Taiwan. Tectonophysics 692, 325–341.

Lehu, R., Lallemand, S., Hsu, S.-K., Babonneau, N., Ratzov, G., Lin, A.T., Dezileau, L., 2015. Deep-sea sedimentation offshore eastern Taiwan: Facies and processes characterization. Mar. Geol. 369, 1–18.

Lehu, R., Lallemand, S., Ratzov, G., Babonneau, N., Hsu, S.-K., Lin, A.T., Dezileau, L., 2016. An attempt to reconstruct 2700 years of seismicity using deep-sea turbidites offshore eastern Taiwan. Tectonophysics 692, 309–324.

Li, C., Shi, X., Kao, S., Chen, M., Liu, Y., Fang, X., Lü, H., Zou, J., Liu, S., Qiao, S., 2011. Clay mineral composition and their sources for the fluvial sediments of Taiwanese rivers. Chin. Sci. Bull. 57, 673–681.

Lin, C.-C., Lin, A.T.-S., Liu, C.-S., Horng, C.-S., Chen, G.-Y., Wang, Y., 2014. Canyon-infilling and gas hydrate occurrences in the frontal fold of the offshore accretionary wedge off southern Taiwan. Mar. Geophys. Res. 35, 21–35.

Liu, J.T., Liu, K.-J., Huang, J.C., 2002. The effect of a submarine canyon on the river sediment dispersal and inner shelf sediment movements in southern Taiwan. Mar. Geol. 181, 357–386.

Liu, Z., Colin, C., Huang, W., Chen, Z., Alain, T., Chen, J., 2007a. Clay minerals in surface sediments of the Pearl River drainage basin and their contribution to the South China Sea. Chin. Sci. Bull. 52, 1101–1111.

Liu, Z., Colin, C., Huang, W., Le, K., Tong, S., Chen, Z., Alain, T., 2007b. Climatic and tectonic controls on weathering in South China and Indochina Peninsula: Clay mineralogical and geochemical investigations from the Pearl, Red, and Mekong drainage basins. Geochem. Geophys. Geosyst. 80.

Liu, J.P., Liu, C.S., Xu, K.H., Milliman, J.D., Chiu, J.K., Kao, S.J., Lin, S.W., 2008a. Flux and fate of small mountainous rivers derived sediments into the Taiwan Strait. Mar. Geol. 256, 65–76.

Liu, Z., Tuo, S., Colin, C., Liu, J.T., Huang, C.-Y., Selvaraj, K., Chen, C.-T.A., Zhao, Y., Siringan, F.P., Boulay, S., Chen, Z., 2008b. Detrital fine-grained sediment contribution from Taiwan to the northern South China Sea and its relation to regional ocean circulation. Mar. Geol. 255, 149–155.

Liu, Z., Zhao, Y., Colin, C., Siringan, F.P., Wu, Q., 2009. Chemical weathering in Luzon, Philippines from clay mineralogy and major-element geochemistry of river sediments. Appl. Geochem. 24, 2195–2205.

Liu, J., Chen, M., Chen, Z., Yan, W., 2010a. Clay mineral distribution in surface sediments of the South China Sea and its significance for sediment sources and transport. Chin. J. Oceanol. Limnol. 28, 407–415.

Liu, Z., Colin, C., Li, X., Zhao, Y., Tuo, S., Chen, Z., Liu, J., Huang, C.-Y., You, C.-F., Huang, K.-F., 2010b. Clay mineral distribution in surface sediments of the northeastern South China Sea and surrounding fluvial drainage basins: source and transport. Mar. Geol. 277, 48–60.

Liu, J.T., Hsu, R.T., Hung, J.-J., Chang, Y.-P., Wang, Y.-H., Rendle-Bühring, R.H., Lee, C.-L., Huh, C.-A., Yang, R.J., 2016a. From the highest to the deepest: the Gaoping River–Gaoping Submarine Canyon dispersal system. Earth Sci. Rev. 153, 274–300.

Liu, Z., Zhao, Y., Colin, C., Stattegger, K., Wiesner, M.G., Huh, C.-A., Zhang, Y., Li, X., Sompongchaiyakul, P., You, C.-F., Huang, C.-Y., Liu, J.T., Siringan, F.P., Le, K.P., Sathiamurthy, E., Hantoro, W.S., Liu, J., Tuo, S., Zhao, S., Zhou, S., He, Z., Wang, Y., Bunsomboonsakul, S., Li, Y., 2016b. Source-to-sink transport processes of fluvial sediments in the South China Sea. Earth Sci. Rev. 153, 238–273.

Malavieille, J., Lallemand, S.E., Dominguez, S., Deschamps, A., Lu, C.-Y., Liu, C.-S., Schnuerle, P., Angelier, J., Collot, J.Y., Deffontaines, B., Fournier, M., Hsu, S.K., Le Formal, J.P., Liu, S.Y., Sibuet, J.C., Thareau, N., Wang, F., the, A.C.T.S.C., 2002. Arc-continent collision in Taiwan: New marine observations and tectonic evolution. In: Byrne, T.B., Liu, C.-S. (Eds.), Geology and Geophysics of an Arc-Continent Collision. Taiwan, Geological Society of America, p. 0.

McLennan, S., 1993. Weathering and global denudation. J. Geol. 101, 295–303.

Mensah, V., Jan, S., Chang, M.-H., Yang, Y.-J., 2015. Intraseasonal to seasonal variability of the intermediate waters along the Kuroshio path east of Taiwan. J. Geophys. Res. Oceans 120, 5473–5489.

Milliman, J.D., Syvitski, J.P.M., 1992. Geomorphic/tectonic control of sediment discharge to the ocean: the importance of small mountainous rivers. J. Geol. 100, 525–544.

Milliman, J.D., Farnsworth, K.L., Albertin, C.S., 1999. Flux and fate of fluvial sediments leaving large islands in the East Indies. J. Sea Res. 41, 97–107.

Molnar, P., 2004. Late cenozoic increase in accumulation rates of terrestrial sediment: how might climate change have affected erosion rates? Annu. Rev. Earth Planet. Sci. 32, 67–89.

Nan, F., Xue, H., Yu, F., 2015. Kuroshio intrusion into the South China Sea: a review. Prog. Oceanogr. 137, 314–333.

Peizhen, Z., Molnar, P., Downs, W.R., 2001. Increased sedimentation rates and grain sizes 2-4 Myr ago due to the influence of climate change on erosion rates. Nature 410, 891–897.

Reiners, P.W., Ehlers, T.A., Mitchell, S.G., Montgomery, D.R., 2003. Coupled spatial variations in precipitation and long-term erosion rates across the Washington Cascades. Nature 426, 645–647.

Selvaraj, K., Lee, T.Y., Yang, J.Y.T., Canuel, E.A., Huang, J.C., Dai, M., Liu, J.T., Kao, S.J., 2015. Stable isotopic and biomarker evidence of terrigenous organic matter export to the deep sea during tropical storms. Mar. Geol. 364, 32–42.

Singh, M., Sharma, M., Tobschall, H., 2005. Weathering of the Ganga alluvial plain, northern India: Implications from fluvial geochemistry of the Gomati River. Appl. Geochem. 20, 1–21.

Sparkes, R.B., Lin, I.-T., Hovius, N., Galy, A., Liu, J.T., Xu, X., Yang, R., 2015. Redistribution of multi-phase particulate organic carbon in a marine shelf and canyon system during an exceptional river flood: Effects of Typhoon Morakot on the Gaoping River–Canyon system. Mar. Geol. 363, 191–201.

Stow, D.A., Tabrez, A.R., 1998. Hemipelagites: Processes, Facies and Model, 129. Special Publications, London, pp. 317–337.

Su, C.-C., Hsu, S.-T., Hsu, H.-H., Lin, J.-Y., Dong, J.-J., 2018. Sedimentological characteristics and seafloor failure offshore SW Taiwan. Terr. Atmos. Ocean. Sci. 29, 65–76.

Summerfield, M., Hulton, N., 1994. Natural controls of fluvial denudation in major world basins. J. Geophys. Res. 99, 13871.

Wan, S., Li, A., Clift, P.D., Stuut, J.-B.W., 2007. Development of the East Asian monsoon: Mineralogical and sedimentologic records in the northern South China Sea since 20 Ma. Palaeogeogr. Palaeoclimatol. Palaeoecol. 254, 561–582.

Wan, S., Li, A., Clift, P.D., Wu, S., Xu, K., Li, T., 2010. Increased contribution of terrigenous supply from Taiwan to the northern South China Sea since 3Ma. Mar. Geol. 278, 115–121.

Wang, Y., Fan, D., Liu, J.T., Chang, Y., 2016. Clay-mineral compositions of sediments in the Gaoping River-Sea system: Implications for weathering, sedimentary routing and carbon cycling. Chem. Geol. 447, 11–26.

Yu, S.-W., Tsai, L.L., Talling, P.J., Lin, A.T., Mii, H.-S., Chung, S.-H., Horng, C.-S., 2017. Sea level and climatic controls on turbidite occurrence for the past 26kyr on the flank of the Gaoping Canyon off SW Taiwan. Mar. Geol. 392, 140–150.

Yuan, D., Han, W., Hu, D., 2006. Surface Kuroshio path in the Luzon Strait area derived from satellite remote sensing data. J. Geophys. Res. Oceans 111.

Zhang, Y., Liu, Z., Zhao, Y., Colin, C., Zhang, X., Wang, M., Zhao, S., Kneller, B., 2018. Long-term in situ observations on typhoon-triggered turbidity currents in the deep sea. Geology 46, 675–678.